Electronic Communication through π-Conjugated Wires in Covalently Linked Porphyrin/C_{60} Ensembles

Gema de la Torre,[a] Francesco Giacalone,[a] José L. Segura,[a] Nazario Martín,*[a] and Dirk M. Guldi*[b]

Abstract: Novel photo- and electroactive triads, in which π-conjugated *p*-phenylenevinylene oligomers (oPPVs) of different length are connected to a photoexcited-state electron donor (i.e., zinc tetraphenylporphyrin) and an electron acceptor (i.e., C_{60}), were designed, synthesized, and tested as electron-transfer model systems. A detailed physicochemical investigation, concentrating mainly on long-range charge separation and charge recombination and kinetics, revealed small attenuation factors β of 0.03 ± 0.005 Å^{-1}. Energy matching between the HOMO levels of C_{60} and oPPVs emerged as a key parameter for supporting molecular-wire-like behavior: It favors rapid and efficient electron or hole injection into the oPPV wires. Large electronic coupling values were determined as a result of paraconjugation in the oPPV moieties.

Keywords: conjugation · electron transfer · fullerenes · molecular wires · porphyrins

Introduction

The rational design of molecular-sized materials for electronic and photonic applications is currently a topic of great interest. In particular, the preparation and integration of multifunctional molecules into architectures of higher order—the so-called bottom-up approach—is the basis for the realization of molecular-scale electronics.[1]

In this context, understanding and testing molecular wires is at the forefront of science, since they provide the ultimate means for electron transport.[2] Among many examples, π-conjugated oligomers are promising prototypes for molecular wires. An important aspect for the use of π-conjugated oligomers is that their chemical properties can be tailored by controlling their length and constitution.[3] Oligo-*p*-phenylenevinylenes (oPPVs) have been successfully used as molecular wires. Recently, energy matching between the donor and bridge units has been recognized as an indispensable requirement for guaranteeing wire behavior.[4]

We have demonstrated wirelike behavior in a series of soluble and fully conjugated oPPVs covalently connected to a C_{60} electron acceptor and to an extended tetrathiafulvalene (exTTF) electron donor (C_{60}-oPPV-exTTF) over distances of 40 Å and beyond. Especially important for an exceptionally small attenuation factor of $\beta = 0.01 \pm 0.005$ Å^{-1} is that the energies of the C_{60} HOMOs match those of the long oPPVs. This facilitates electron/hole injection into the wire. Equally important is strong electronic coupling, realized through the paraconjugation of the oPPVs into the exTTF electron donor, which leads to donor–acceptor coupling constants V in $C_{60}^{\bullet-}$-oPPV-exTTF$^{\bullet+}$ of about 5.5 cm^{-1} and assists charge-transfer reactions that exhibit a rather weak dependence on distance.[5]

Porphyrins are naturally occurring light-harvesting building blocks. Rich and extensive absorptions (i.e., π–π* transitions) hold particular promise for increased absorptive cross sections and thus efficient use of the solar spectrum. Their excited-state properties are fine-tuned by varying the central metal ion and the substituents at the peripheral *meso* or β positions.[6] Typically, high electronic excitation energies (>2.0 eV) power a strongly exergonic electron transfer, which subsequently intercedes the conversion between light and chemical/electrical energy. Fullerenes, on the other hand, are three-dimensional electron acceptors that exhibit small reorganization energies in electron-transfer processes.

[a] Dr. G. de la Torre, Dr. F. Giacalone, Dr. J. L. Segura, Prof. Dr. N. Martín
Departamento Química Orgánica
Facultad de Ciencias Químicas
Universidad Complutense, 28040-Madrid (Spain)
Fax: (+34) 913-944-103
E-mail: nazmar@quim.ucm.es

[b] Prof. Dr. D. M. Guldi
Friedrich-Alexander-Universität Erlangen-Nürnberg
Institute for Physical Chemistry
Egerlandstrasse 3, 91058 Erlangen (Germany)
Fax: (+49) 9131-852-8307
E-mail: dirk.guldi@chemie.uni-erlangen.de

 DOI: 10.1002/chem.200400604

To achieve ultrafast charge separation while retarding charge-recombination processes, these aspects are of central importance.[7] The ZnP/C_{60} couple has emerged as an important benchmark in unraveling the complexity of electronic interactions occurring in photosynthesis and in model systems.[8–10]

Here we present a full account on two novel donor–bridge–acceptor systems with C_{60} and zinc(II) tetraphenylporphyrin (ZnP) as photo- and redox-active components. The two moieties are covalently connected through soluble oPPVs of different length, that is, a molecular trimer and pentamer. To the best of our knowledge this is the first example in which both ZnP and C_{60} units are connected by oPPVs.[11] The design and study of these novel compounds, ZnP-oPPV(3)-C_{60} (**13a**) and ZnP-oPPV(5)-C_{60} (**13b**) allows an evaluation of the impact that structural parameters have on the following aspects:

1) The consequences for electronic communication.
2) The effect of the length of the oPPV spacer on the energy- and electron-transfer mechanism.
3) The torsional mobility of the porphyrin about the phenyl ring connected to the oPPV spacer.
4) Most importantly, the molecular-wire behavior.

Results

Synthesis and characterization: Scheme 1 summarizes the preparation of target ZnP-oPPV-C_{60} triads **13a**,**b** and ZnP-

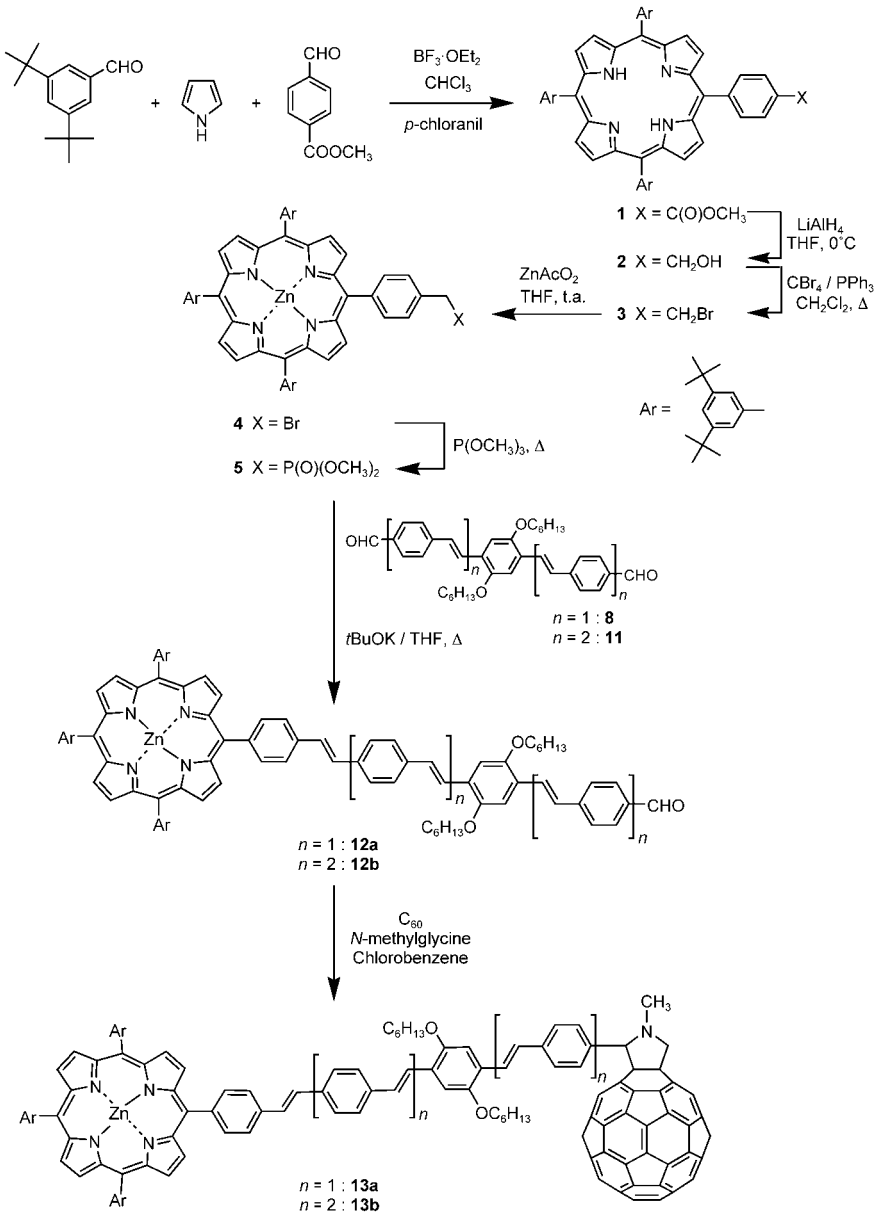

Scheme 1. Synthesis of the novel triads **13a**,**b**.

Abstract in Spanish: *En el presente artículo se describen el diseño, síntesis y estudio de la transferencia electrónica de nuevas triádas foto y electroactivas utilizadas como sistemas modelo. Estos sistemas están constituidos por oligómeros π-conjugados derivados del p-fenilenvinileno (oPPVs) de distinta longitud conectados a un dador electrónico con estado excitado (i.e. tetrafenilporfirina de zinc) y un aceptor electrónico (i.e. C_{60}). El estudio físico-químico detallado, centrado fundamentalmente en los procesos de separación de carga a larga distancia y los procesos y cinética de recombinación, revela valores del factor de atenuación (β) de 0.03± 0.005 $Å^{-1}$. La concordancia energética entre los niveles HOMO de C_{60} y de oPPV se ha revelado como un parámetro fundamental para confirmar el comportamiento de cable molecular: se favorece una rápida y eficiente inyección de electrones o huecos en los cables de oPPV. Se han determinado valores de acoplamiento electrónico elevados como consecuencia de la paraconjugación presente en las unidades de oPPV.*

oPPV references **12a**,**b**. Zinc porphyrin (ZnP) was prepared by using the Lindsey methodology.[12] Pyrrole and a 3:1 mixture of 3,5-di-*tert*-butylbenzaldehyde[13] and methyl 4-formylbenzoate were condensed in the presence of $BF_3{\cdot}OEt_2$, followed by oxidation with *p*-chloranil, to yield porphyrin **1**[14] in 14% (Scheme 1). In the next step, conversion of the ester functionality to a bromomethyl moiety was achieved by reduction with $LiAlH_4$ in THF and bromination with CBr_4 in the presence of PPh_3. The overall yield was 73%.[15] Quantitative metalation of **3** with $Zn(OAc)_2$ afforded zinc(II) porphyrin **4**, and subsequent treatment with $P(OMe)_3$ led to dimethylphosphonate derivative **5**. The single chromophore Zn^{II} tetrakis(di-*tert*-butylphenyl)porphyrinate (**ZnTTP**) was also prepared as a reference compound.

ZnP-oPPV systems **12a** and **12b** were synthesized by Wadsworth–Emmons olefination between phosphonatoporphyrin **5** and oligomers **8** and **11** (Scheme 1), carrying two formyl moieties. The reaction between **5** and equimolar amounts of **8** or **11** in the presence of potassium *tert*-butoxide afforded **12a** and **12b** in about 45% yield. Additionally, certain amounts of the symmetrical ZnP-oPPV-ZnP systems were isolated.[16]

Compounds **12a** and **12b** are suitable starting materials for the synthesis of target molecules **13a** and **13b**, which were prepared by 1,3-dipolar cycloaddition between **12a** or **12b**, *N*-methylglycine, and C_{60} in chlorobenzene in 51 and 32% yield, respectively. Since the reaction takes place by cycloaddition of in-situ-generated azomethyne ylides to C_{60}, it creates a chiral center at the fulleropyrrolidine ring.[17] Consequently, **13a** and **13b** were isolated as racemic mixtures.

The synthesis of oligomers **8** and **11a**,**b** was carried out according to a previously reported procedure (Scheme 2).[18] It proceeds through sequential Wadsworth–Emmons reaction between phosphonate- and formyl-containing subunits. The reaction between 2,5-bis(dimethylphosphonatomethyl)-1,4-dihexyloxybenzene[19] (**6**) and the mono(diethylacetal) of terephthaldehyde (**7**), followed by acidic treatment, afforded trimer **8**. Condensation of **8** and **9** then leads to pentamer **10**, which was reduced with DIBAL-H (2:1 stoichiometry) to the desired dialdehyde-containing pentamer **11a** (54%), together with the monoformylated pentamer **11b**, which was obtained in a lower yield (12%).[20]

All structures were confirmed by spectroscopic analyses (NMR, FTIR, and MS). ^{1}H NMR spectra of **12a**,**b** and **13a**,**b** show signals at around $\delta = 9$ ppm for the pyrrolic protons of the porphyrin core. The pyrrolidine signature appears between $\delta = 4.7$ and 3.9 ppm as two doublets (AB system) and one singlet. High-resolution ^{1}H NMR spectra reveal a *trans* configuration of the vinyl protons of the oligomer moiety and thus confirm the stereoselectivity of the Wadsworth–Emmons reaction. The absorption spectrum of **13b** in dichloromethane (Figure 1a) represents a linear

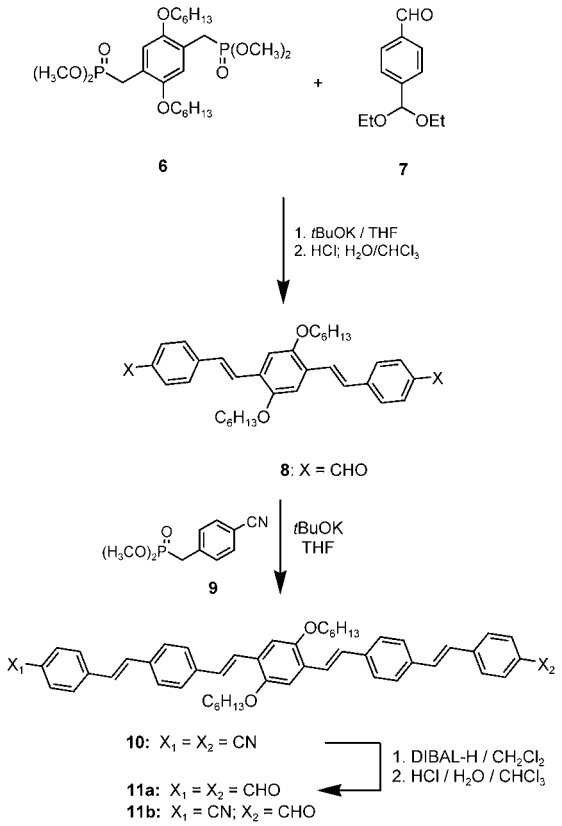

Scheme 2. Synthesis of oPPVs **8** and **10**.

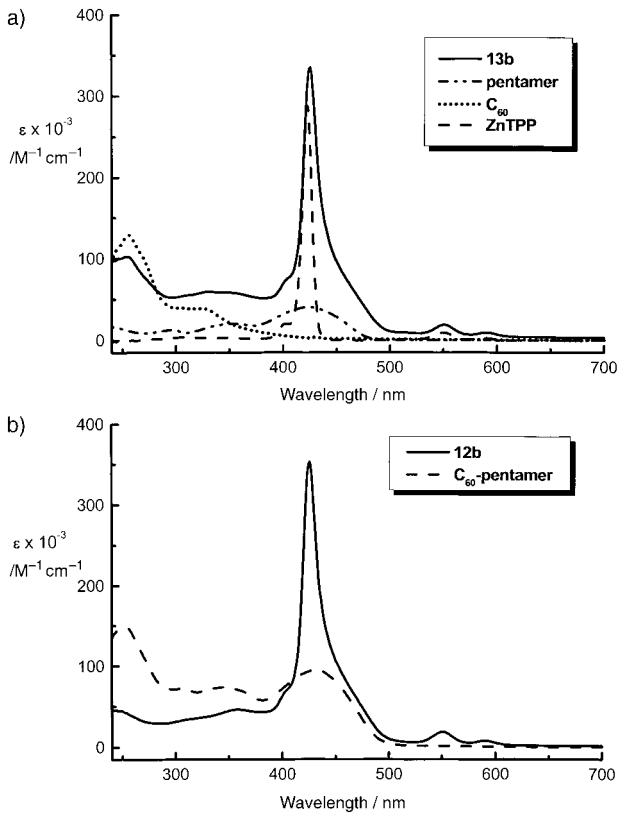

Figure 1. a) UV/Vis spectra of **13b** and its molecular components **ZnTPP**, **pentamer**, and C_{60} (*N*-methylfulleropyrrolidine) used as reference. b) UV/Vis spectra of **12b** and **C_{60}-pentamer** in dichloromethane.

combination of the spectra of **ZnTPP**, **pentamer**, and C_{60}. A similar trend is seen in **12b** and **C_{60}-pentamer** (see Figure 1b).

Dyads **17** and **18** were synthesized, as reference compounds for photophysical studies (see below), from the respective monoformylated oligomers **11b** and **16** by following the typical Prato procedure for the preparation of fulleropyrrolidines (Scheme 3). Trimer **16** had not been previously reported in the literature, and it was obtained in a two-step procedure from phosphonate **6** and benzaldehyde (**14**) under basic conditions with careful control of the stoichiometry (**6**/**14** 2/1). Further treatment of the resulting stilbene derivative **15** with commercially available diethyl ketal **7** and subsequent acidic treatment afforded trimer **16** endowed with a formyl group (see Experimental Section).

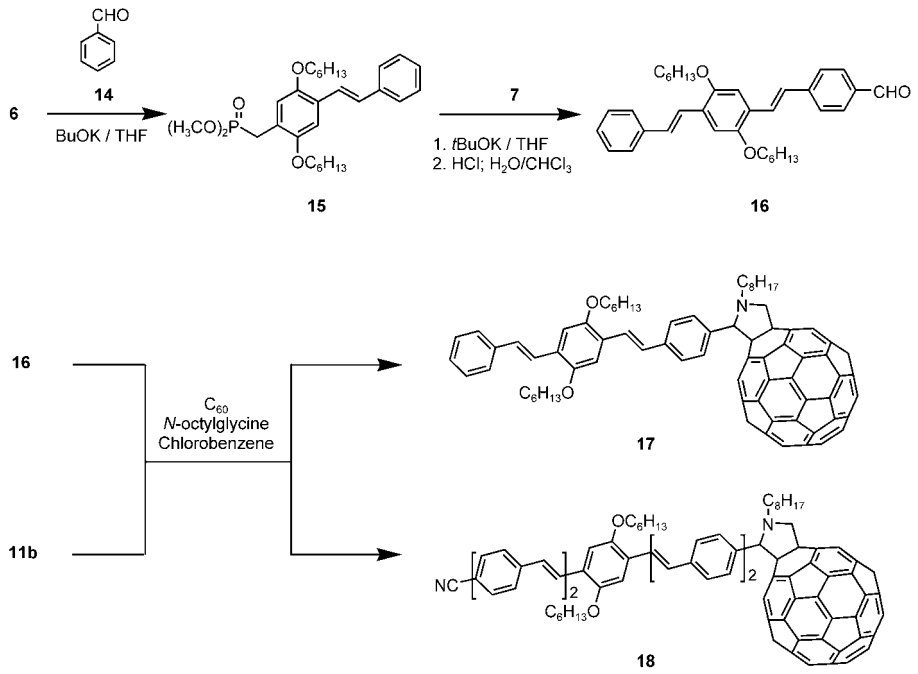

Scheme 3. Synthesis of oPPVs **16** and reference compounds **17** and **18**.

Electrochemistry: The electrochemical features of **13a** and **13b** were probed by cyclic voltammetry at room temperature. Their redox potentials are collected in Table 1, along with those of **ZnTPP**, **C_{60}**, **trimer** (**8**: X = −H), and **pentamer** (**10**: $X_1 = X_2 = H$) as references.

Compounds **13a**,**b** show an amphoteric redox behavior with waves at both oxidation and reduction sides. They exhibit four oxidation waves at potentials similar to those found for the oxidation of **ZnTPP** and **8** (X = H)/**10** ($X_1 = X_2 = H$). Only the first and third oxidation processes are quasireversible, which leads to their assignment to ZnP oxidation. The second and fourth oxidation steps are irreversible and correspond to oligomer-centered events (see Table 1).

The reduction scan of the cyclic voltammograms is dominated by four quasireversible C_{60} reduction waves. These appear together with two ZnP reduction steps and yet another reduction wave at around −1.90 V, which reflects the first reduction wave of the oligomer unit.

Theoretical calculations: Theoretical calculations were performed at the semiempirical PM3 level to determine the geometries of **13a**,**b** (Figure 2). All the predicted geometrical values were found to be in good agreement with the experimental data.[21]

Photophysics: All reference compounds emit fluorescence in different spectral regions of the solar spectrum and with drastically different quantum yields. In decreasing order, fluorescence maxima were observed at 445 nm (**trimer**) > 485 (**pentamer**) > 605 (**ZnTPP**) > 715 nm (**C_{60}**). A summary of the fluorescence spectra is shown in Figure 3 for toluene as solvent. While the fluorescence quantum yields still follow the same trend—0.75 (**trimer**) > 0.5 (**pentamer**) > 4×10^{-2} (**ZnTPP**)[22] > 6×10^{-4} (**C_{60}**)[23]—the corresponding lifetimes diverge substantially from both of these trends. In particular, the lifetimes lie between 2.7 and 0.8 ns for **ZnTPP** and **pentamer**, respectively.

Characteristic transient singlet and triplet spectra were recorded in the pico-, nano-, and microsecond time regimes. Typically, in our ultrafast experiments (20 ps laser pulses)

Table 1. Redox potentials in *o*-dichlorobenzene/MeCN (4/1).[a]

Compound	E^1_{pa}	E^2_{pa}	E^3_{pa}	E^4_{pa}	E^1_{pc}	E^2_{pc}	E^3_{pc}	E^4_{pc}	E^5_{pc}
ZnTPP	0.84	1.23	–	–	−1.42	−1.78	–	–	–
C_{60}	–	–	–	–	−0.59	−1.01	−1.47	−1.94	–
trimer	1.11	1.27	1.53	2.03	–	–	–	–	–
pentamer	0.99	1.28	1.41	1.74	–	–	–	–	−1.94
13a	0.83	1.05	1.24	1.39	−0.61	−1.02	−1.62	−2.05	−1.28 ZnP −1.79 ZnP −1.88 olig
13b	0.82	0.94	1.22	1.43	−0.62	−1.02	−1.65	−2.10	−1.26 ZnP −1.90 olig

[a] V versus SCE; glassy carbon working electrode; Ag/Ag^+ reference electrode; Pt counterelectrode; 0.1 M Bu_4NClO_4; scan rate: 200 mV s^{-1}; concentrations: $0.5–2.0\times10^{-3}$ M.

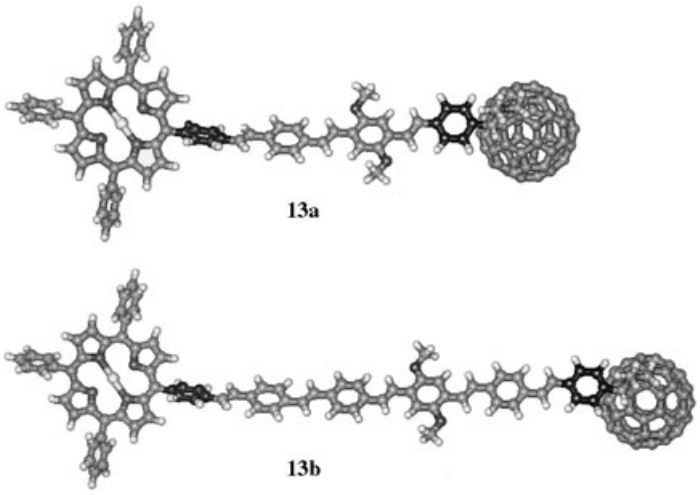

Figure 2. Minimum energy calculated structures (PM3) for **13a** and **13b**. Hexyl and *tert*-butyl groups were removed for the computational study.

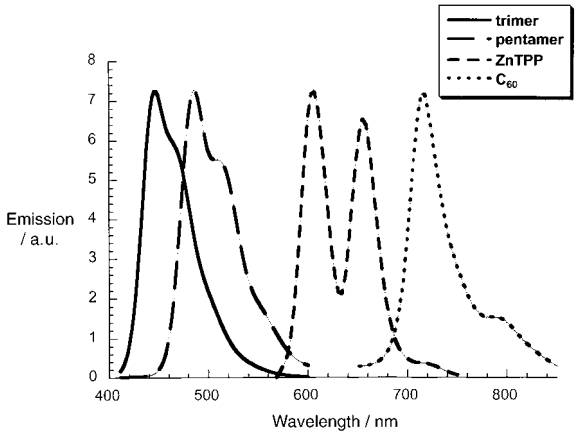

Figure 3. Room-temperature fluorescence spectra of **trimer**, **pentamer**, **ZnTTP**, and $\mathbf{C_{60}}$ building blocks, recorded on toluene solutions that exhibit optical absorptions of 0.5 at the 400 nm excitation wavelength. The spectra are normalized to show similar fluorescence intensities at their maxima.

we see singlet excited states that are formed instantaneously, that is, with kinetics faster than $5\times10^{10}\,s^{-1}$. In the **trimer**, **pentamer**, and **ZnTPP** references new singlet–singlet absorptions develop, which are red-shifted relative to the ground-state transition. These ground-state transitions appear in the differential absorption spectra as bleaching, that is, loss in relative amplitude when photoexcited. For example, in **ZnTPP** singlet–singlet maxima are seen at 500 and 615 nm relative to the minima of the ground-state transitions at 425 and 550 nm. A representative picosecond time-resolved absorption spectra, taken after a 20 ps laser pulse at 532 nm in toluene solution for **ZnTPP**, is displayed in Figure 4.

Fast intersystem crossing ($k_{isc}\approx10^8\,s^{-1}$, Figure 4b) governs the fate of the metastable singlet excited states in all building blocks. The corresponding triplet–triplet absorptions of

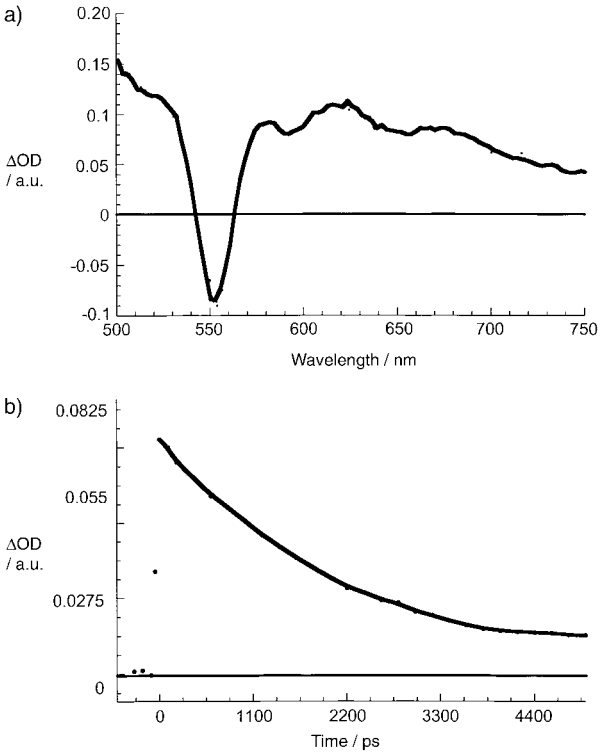

Figure 4. a) Differential absorption spectrum (Vis) obtained upon picosecond flash photolysis (532 nm) of ca. 1.0×10^{-5} M solutions of **ZnTPP** building block in nitrogen-saturated toluene with a time delay of 50 ps at room temperature. The spectrum corresponds to the singlet–singlet spectrum of **ZnTPP**. b) Illustration of the intersystem crossing process in photoexcited **ZnTPP**.

trimer, **pentamer**, **ZnTPP**, and $\mathbf{C_{60}}$ are all located in the range between 500 and 900 nm (Figures 5 and 6). The oxygen-sensitive triplets ($k_{oxygen}\approx10^9\,M^{-1}\,s^{-1}$), with triplet

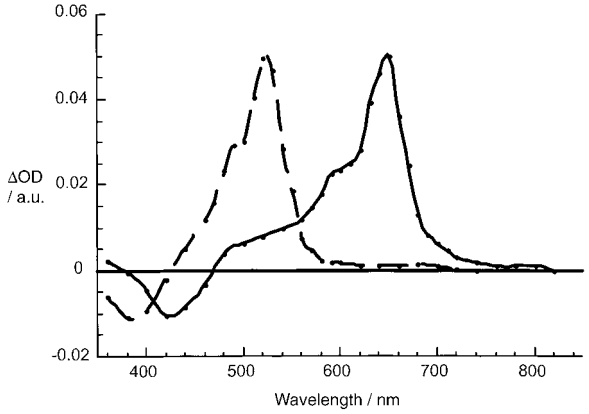

Figure 5. Differential absorption spectrum (Vis and NIR) obtained upon nanosecond flash photolysis (355 nm) of ca. 1.0×10^{-5} M solutions of **trimer** (dashed line) and **pentamer** (solid line) building blocks in nitrogen-saturated toluene with a time delay of 50 ns at room temperature. The spectra correspond to the triplet–triplet spectra of both building blocks.

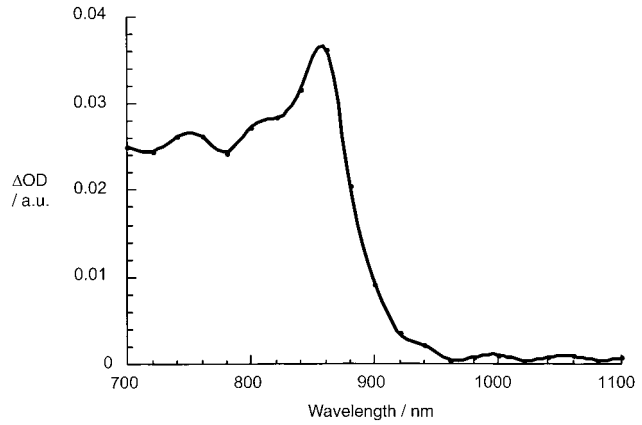

Figure 6. Differential absorption spectrum (NIR) obtained upon nanosecond flash photolysis (355 nm) of ca. 1.0×10^{-5} M solutions of **12b** in nitrogen-saturated toluene with a time delay of 50 ns at room temperature. The spectrum corresponds to the triplet–triplet spectrum of the ZnP chromophore.

lifetimes longer than 20 μs, are formed with quantum yields of 0.98 (**C_{60}**) > 0.88 (**ZnTPP**) > 0.2 (**pentamer**).

ZnP-trimer and ZnP-pentamer precursors: Next we investigated the ZnP/oligomer interactions in the ZnP-trimer (**12a**) and ZnP-pentamer (**12b**) precursors. In the ground state, features of both components are discernable. The porphyrin transitions are sharp (Soret-band: 427 nm; Q-band: 550 and 590 nm) and dominate most of the absorption spectrum. Those of the oligomeric wires are broad (Figure 1b). When the spectra of the **ZnTPP**/oligomer building blocks are compared with those of **12a** and **12b**, no notable perturbations or alterations of the spectra are seen. The spectra of **12a** and **12b** appear as the simple sum of the two component spectra.

The characteristic fluorescence of the oligomeric wire proved to be a more useful probe for electronic interactions (excitation around 350 nm). In the 400–600 nm region, the strong emission of the oligomeric wires, with maxima at 445 nm (**trimer**: 2.78 eV) and 485 nm (**pentamer**: 2.55 eV), are seen for the building blocks. When ZnP is present, strong fluorescence quenching, with quenching factors of about 500 (Φ values in toluene: **12a**: 4.8×10^{-4}; **12b**: 1.6×10^{-3}), indicates almost instantaneous deactivation of the photoexcited oligomer. Importantly, solvents of different polarity (i.e., toluene, THF, and benzonitrile) had virtually no impact on the fluorescence quenching, and this supports a deactivation by energy transfer.[24]

In parallel experiments we excited the ZnP chromophore at 427 nm or 550 nm and compared **ZnTPP** with **12a** and **12b**. Here no differences were found for the high-energy emission (2.05 eV) with quantum yields of about 4×10^{-2}. Also, the ZnP fluorescence lifetime of 2.0 ± 0.2 ns remains virtually indistinguishable in the different samples.

In time-resolved experiments, the only notable photoproduct on the nano- to microsecond timescale is the ZnP triplet excited state (1.5 eV).[25] An example of a spectrum is shown in Figure 6. The characteristic triplet–triplet fingerprint around 860 nm is formed in nearly quantitative yield (> 90 %).

Independent of which part of **12a** or **12b** is photoexcited, that is, either the ZnP chromophore or the oligomeric wire, singlet and triplet excited states both reside on the ZnP moiety. Figure 7 summarizes the different pathways.

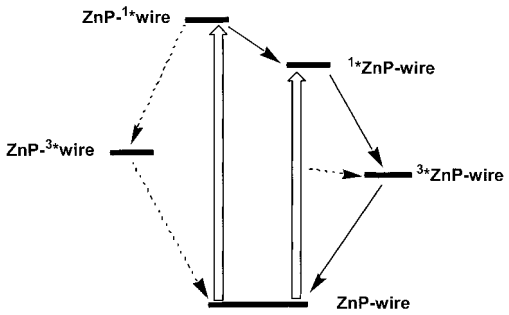

Figure 7. Energy levels of excited states in **ZnP-trimer** (**12a**) and **ZnP-pentamer** (**12b**); solid arrows indicate major pathways.

Trimer-C_{60} and pentamer-C_{60} precursors: The relative weak absorptions of C_{60} in the **trimer-C_{60}** and **pentamer-C_{60}** precursors (see Figure 1b) limit the fluorescence experiments to probing the oligomeric part. In a typical experiment, with 400–420 nm excitation wavelength, the photoexcited oligomer is deactivated almost instantaneously. This is evidenced by 1) fluorescence quantum yields of 6.0×10^{-4} (Figure 8) or

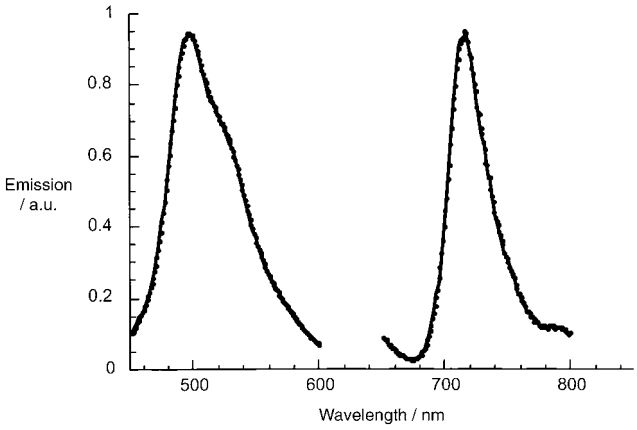

Figure 8. Room-temperature fluorescence spectra of **pentamer-C_{60}** (**18**) recorded with a toluene solution that exhibits an optical absorption of 0.5 at the 400 nm excitation wavelength. The quantum yields of both photoexcited species (i.e., pentamer and C_{60}) are 6×10^{-4}.

less and 2) the lack of any measurable fluorescence lifetimes exceeding the 100 ps time window of our instrumental resolution.

Concurrent with the disappearance of the oligomer fluorescence in the visible region of the spectrum (400–600 nm),

we noted the appearance of the C_{60} emission in the near-infrared (650–800 nm) with a maximum at 720 nm (see Figure 8).[23] Moreover, the C_{60} fluorescence quantum yields match that determined for **C_{60}**. Fluorescence quantum yields around $6 \pm 0.1 \times 10^{-4}$ illustrate this trend, despite the near exclusive excitation of the oligomer moieties. Additional excitation spectra of the C_{60} fluorescence, which reveal the ground-state transitions of **trimer** and **pentamer**, led us to postulate an efficient and quantitative transfer of singlet excited state energy from the highly energetic oligomer singlet excited state (2.5–2.8 eV) to the low-lying singlet excited state of C_{60} (1.76 eV).[26]

In time-resolved fluorescence experiments the only detectable fluorescence was that of C_{60}. Again, its lifetime (ca. 1.5 ns) is identical to that found for **C_{60}**. No residual traces of the long-lived oligomer fluorescence were noted. This suggests that the strong C_{60}/oligomer coupling causes extremely fast intramolecular singlet–singlet energy-transfer dynamics ($>10^{10}$).

Time-resolved transient absorption measurements further corroborated the fluorescence experiments. In picosecond experiments, the singlet excited states of C_{60} (1.76 eV) and of the oligomer (ca. 2.5 eV) are populated, due to their overlapping absorption in this spectral region (see Figure 1). The relative absorption ratio of C_{60}/oligomer is about 1/4 at 355 nm. Instead of showing the strong oligomer singlet–singlet transitions, the transient spectra, recorded immediately after the 20 ps laser pulse, show mainly a broad 880 nm peak (not shown). This maximum corresponds to the singlet–singlet fingerprint seen upon exclusive **C_{60}** excitation. This supports our earlier notion that a rapid intramolecular transduction of energy funnels the excited-state energy to the fullerene core to generate ^{1}*C_{60} with quantum yields of nearly unity.[27]

Again, the C_{60} singlet growth kinetics could not be resolved within our time resolution of about 20 ps. Once formed, the singlet–singlet transitions are metastable and decay with monoexponential dynamics ($5.0 \pm 0.5 \times 10^8$ s^{-1}) to generate the triplet manifold. Spectral characteristics of the latter, as recorded at the conclusion of the 4000 ps timescale, are transient maxima at 380 nm and 700 nm.[23]

In nanosecond experiments, the only photoproduct found involves the same C_{60} triplet state features. The C_{60} triplet transitions were then employed as convenient markers to quantify the energy-transfer efficiency. In line with the conclusion of the fluorescence experiments, we found in the **trimer-C_{60}** and **pentamer-C_{60}** precursors triplet yields, which are virtually identical to that of C_{60}. This confirms that, regardless of the initially excited state (^{1}*trimer/^{1}*pentamer or ^{1}*C_{60}) the final photoexcited state is the same, namely, ^{3}*C_{60}, formed quantitatively by the indirect (i.e., exciting trimer or pentamer) or direct (i.e., exciting C_{60}) route (see Figure 9).

ZnP-trimer-C_{60} and ZnP-pentamer-C_{60} wires: We focused in our ZnP-trimer-C_{60} (**13a**) and ZnP-pentamer-C_{60} (**13b**) experiments on populating the ZnP excited state exclusively and monitoring its fate.[28] In Figure 10, which summarizes

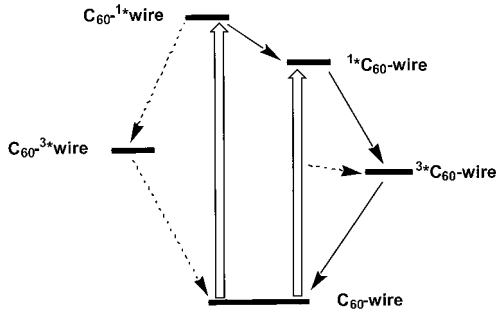

Figure 9. Energy levels of excited states in **trimer-C_{60}** (**17**) and **pentamer-C_{60}** (**18**); solid arrows indicate major pathways.

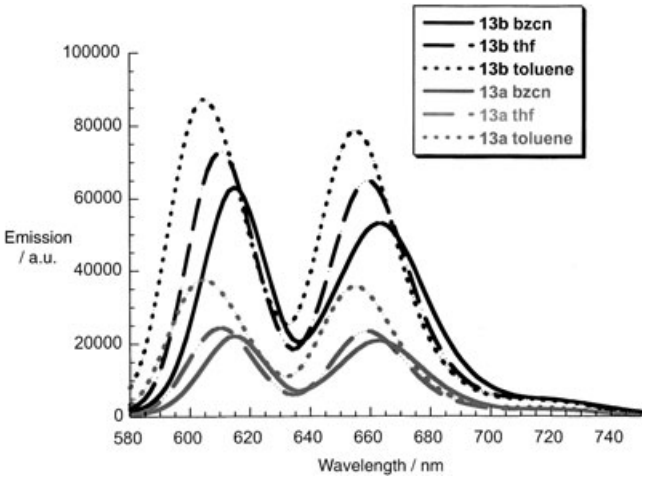

Figure 10. Room-temperature fluorescence spectra of **13a** and **13b**, recorded with solutions that exhibit optical absorptions of 0.5 at the 425 nm excitation wavelength. The fluorescence quantum yields are for **13a**: 0.01 (toluene), 0.006 (THF), 0.005 (benzonitrile), and for **13b**: 0.021 (toluene), 0.018 (THF), 0.015 (benzonitrile).

the steady-state fluorescence experiments, several general trends emerge. First, we see a difference between the trimer and pentamer systems with typical fluorescence yields that are twice as high in the latter (Φ values in toluene: **13a**: 0.010, **13b**: 0.021). At first glance, this observation speaks for a distance-dependent deactivation of the ZnP singlet excited state. Second, fluorescence quenching becomes progressively stronger in the more polar solvents: toluene < THF < benzonitrile, which implies that the driving force for intramolecular electron transfer changes with solvent polarity. Better solvation of radical ions in, for example, benzonitrile, stabilizes the radical ion pair state and, in turn, enhances the free-energy changes for its formation. Third, the emission is red-shifted in THF and benzonitrile, which can be attributed to the coordination of a solvent molecule to the axial position of the zinc center.

Time-resolved fluorescence decay measurements qualitatively support the first and second observations. In particular, fluorescence deactivation in **13a** is faster than in **13b** (0.58 vs 0.28 ns, both in THF) and faster in THF than in benzonitrile (0.28 vs 0.12 ns for **13b**).

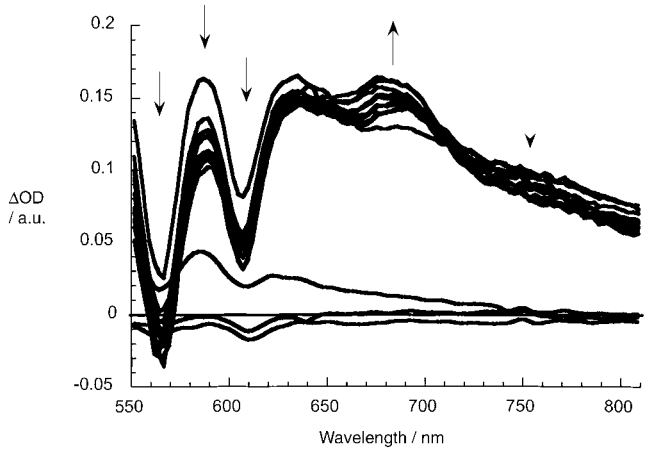

Figure 11. Differential absorption spectra (Vis and NIR) obtained upon picosecond flash photolysis (532 nm) of ca. 1.0×10^{-5} M solutions of **13b** in nitrogen-saturated THF with several time delays between −50 and 4000 ps at room temperature. The spectra correspond to the changes that are associated with the transformation of the ZnP singlet excited state to the radical pair ZnP$^{\bullet+}$-pentamer-$C_{60}^{\bullet-}$.

The fate of ^{1}*ZnP in **13a** and **13b** was also examined by pico-/nano-/microsecond transient absorption spectroscopy. Representative picosecond time-resolved absorption spectra, taken after 532 nm laser excitation of **13b** in THF solution, are displayed in Figure 11.

At early times (50–100 ps), these are practically identical to those of the **ZnTPP** building block, exhibiting strong bleaching at 550 nm (similar to Figure 4) and attesting to formation of the ZnP singlet excited state. At a delay time of about 200 ps, a new transition around 670 nm starts to grow in (Figure 11) together with another absorption in the near-infrared, and their formation is completed around 2000 ps. Based on a spectral comparison, we ascribe the former to the ZnP π radical cation (ZnP$^{\bullet+}$), while the latter band belongs to the fullerene π radical anion ($C_{60}^{\bullet-}$).[23] An important criterion is the kinetic resemblance 1) between the decay of ^{1}*ZnP and the growth of ZnP$^{\bullet+}$/$C_{60}^{\bullet-}$, and 2) between decay/growth and the fluorescence lifetimes. The charge-separation rate of **13a** is 4.5×10^9 s^{-1} in THF and 3.2×10^9 s^{-1} in benzonitrile, while in **13b** it is somewhat slower (3.2×10^9 s^{-1} in THF and 4.5×10^9 s^{-1} in benzonitrile; Table 2). In accordance with these results, we propose that

Table 2. Charge separation and charge recombination dynamics for **13a** and **13b** in different solvents.

	13a		**13b**	
	charge separation	charge recombination	charge separation	charge recombination
THF	4.5×10^9 s^{-1}	1.2×10^6 s^{-1}	3.2×10^9 s^{-1}	9.3×10^5 s^{-1}
benzonitrile	3.2×10^9 s^{-1}	4.4×10^6 s^{-1}	4.5×10^9 s^{-1}	2.7×10^6 s^{-1}

charge separation from the ZnP singlet excited state to the electron-accepting fullerene creates ZnP$^{\bullet+}$/$C_{60}^{\bullet-}$. The formation of ZnP$^{\bullet+}$/$C_{60}^{\bullet-}$ is responsible for the fast deactivation of the photoexcited chromophore. The absorption of the charge-separated ZnP$^{\bullet+}$/$C_{60}^{\bullet-}$ pair is persistent on the picosecond timescale and decays in the nano-/microsecond regime (vide infra). The charge-recombination dynamics were then analyzed by following the absorption changes of the one-electron reduced form of the electron acceptor ($C_{60}^{\bullet-}$) and that of the one-electron oxidized form of the electron donor (ZnP$^{\bullet+}$). An example is shown in Figure 12.

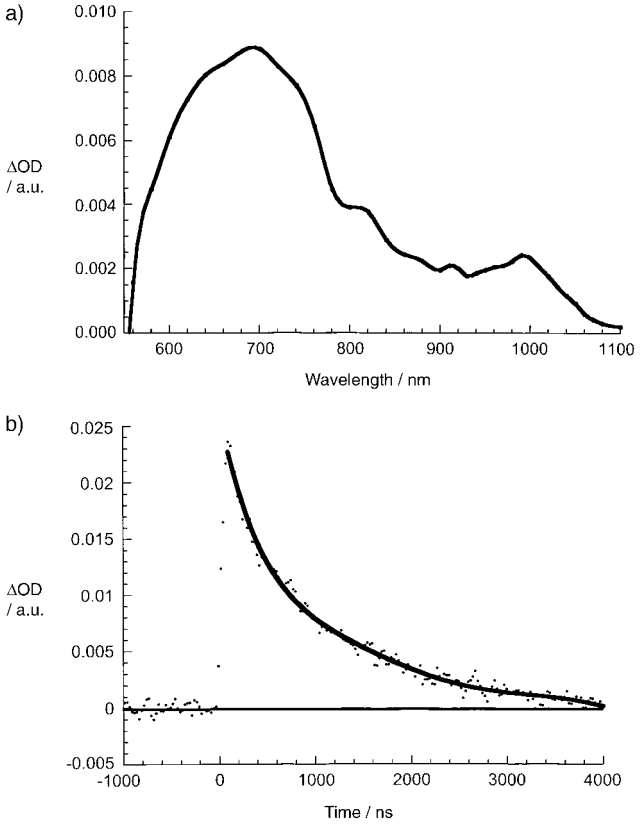

Figure 12. a) Differential absorption spectrum (Vis and NIR) obtained upon nanosecond flash photolysis (532 nm) of ca. 1.0×10^{-5} M solutions of **13b** in nitrogen-saturated THF with a time delay of 100 ns at room temperature. The spectrum corresponds to the radical pair ZnP$^{\bullet+}$-pentamer-$C_{60}^{\bullet-}$. b) Decay of ZnP$^{\bullet+}$-pentamer-$C_{60}^{\bullet-}$ (at 1000 nm).

In oxygen-free solutions, the decays were well fitted by a single exponential expression. For both systems, charge recombination is faster in more polar solvents (**13a**: THF: 1.2×10^6 s^{-1}, benzonitrile: 4.4×10^6 s^{-1}; **13b**: THF: 9.3×10^5 s^{-1}, benzonitrile: 2.7×10^6 s^{-1}). A decrease in $-\Delta G°$ and faster charge-recombination kinetics is a typical phenomenon for the Marcus inverted region, where the electron transfer rates start to decrease with increasing change in free energy.[29]

Discussion

An important fact is that absorption spectroscopy and cyclic voltammetry confirm the lack of significant electronic communication between the constituents (**ZnTPP**, **trimer**, **pen-**

tamer, and $\mathbf{C_{60}}$) in **12a**/**12b** and **13a**/**13b** in their ground state.

The photoreactivity of **12a**/**12b** is rationalized by a thermodynamic evaluation. Among the singlet excited states, the one that is localized on the ZnP moiety has the lowest energy (2.05 eV) and hence evolves as the thermodynamically stabilized intermediate. The same observation must hold for the triplet excited states, although the exact triplet energies of the oligomeric wires are not known, since the only triplet product is that of ZnP.

Formation of radical ion pairs, that is, oxidized ZnP/reduced oligomer (ca. 2.7 eV) or reduced ZnP/oxidized oligomer (ca. 2.6 eV), appears to be uncompetitive (i.e., starting with the trimer or pentamer singlet excited state) or unfeasible (i.e., starting with the ZnP singlet excited state).[30] Moreover, our physicochemical characterization rules out these possibilities. No direct spectroscopic evidence was found for the formation of $ZnP^{\bullet+}$/oligomer$^{\bullet-}$ or $ZnP^{\bullet-}$/oligomer$^{\bullet+}$. The solvent-independent fluorescence quenching of the oligomer emission, as an indirect proof, is also inconsistent with an electron-transfer mechanism.

For photoexcited **trimer-C_{60}** and **pentamer-C_{60}** intramolecular electron transfer, as an alternative deactivation channel, might evolve from the singlet excited state of the oligomers. The energies of the radical ion pair states (ca. 1.8–1.9 eV)[30] lead to a position somewhat higher than that of the C_{60} singlet excited state at 1.76 eV and prevent this reaction pathway. Nevertheless, strictly on the basis of thermodynamic considerations, we would expect the following reaction to occur [Eq. (1)].

$$\mathbf{C_{60}}\text{-}^{1*}\mathbf{wire} \rightarrow \mathbf{C_{60}}^{\bullet-}\text{-}\mathbf{wire}^{\bullet+} \quad (1)$$

In line with a series of previous investigations on several C_{60}/oligomer systems, the more exothermic energy transfer prevails, and this leaves electron-transfer deactivation as an insignificant contribution.[27]

Although all the reference systems (i.e., **12a**, **12b**, **trimer-C_{60}**, and **pentamer-C_{60}**) exhibit energy-transfer deactivation, no energy-transfer activity was noted for ZnP. This is different in **13a**/**13b**. Connecting **ZnTPP** with $\mathbf{C_{60}}$ through **trimer** or **pentamer** results in rapid electron-transfer deactivation. Relative to a previously reported ZnP-C_{60} system,[31] for which rate constants of $8.3\times10^{10}\ s^{-1}$ (charge separation) and $7.7\times10^{9}\ s^{-1}$ (charge recombination) were reported, both processes are notably slower in **13a** and **13b**. Rate constants for charge separation and recombination are about $10^{9}\ s^{-1}$ and about $10^{6}\ s^{-1}$, respectively. Considering the large edge-to-edge distances of 26.1 Å (**13a**) and 39.0 Å (**13b**), such rate constants are only feasible if good electronic coupling between ZnP and C_{60} is guaranteed. In fact, calculations of the electronic coupling matrix element V within the framework of the Marcus electron transfer theory yielded high values.[29] The values of $4.9\ cm^{-1}$ (**13a**) and $4.1\ cm^{-1}$ (**13b**) compare to $1.6\times10^{-4}\ cm^{-1}$ derived for tetrads formed by connected electroactive species (Fc-ZnP-Zn-C_{60}) that span comparable distances.[32] Using an alternative approach, namely, analyzing the $\ln k_{CS}$ versus distance relationship (vide infra), also gave a high value of $2.2\ cm^{-1}$. In summary, fully conjugated oPPVs are good mediators for electronic coupling over large distances.

To analyze the charge-recombination mechanism we probed the radical-pair lifetimes between 268 and 365 K (Figure 13). The Arrhenius plot for **13a** can be separated

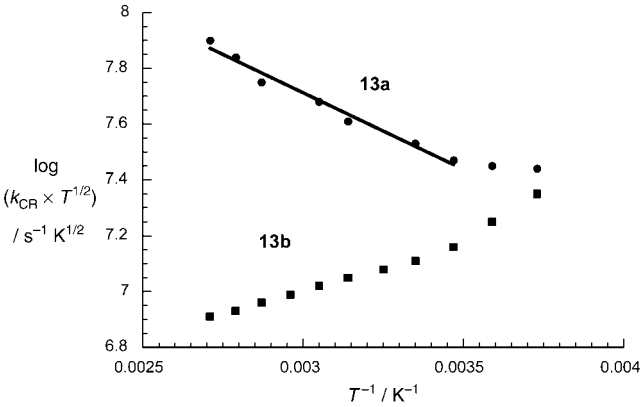

Figure 13. Arrhenius analyses of the temperature-dependent electron-transfer rate constants for **13a** and **13b** in deoxygenated benzonitrile.

into two distinct sections: A low-temperature regime (< 300 K) and a high-temperature regime (> 300 K). The weak temperature dependence in the 268–300 K range suggests that a stepwise intramolecular charge-recombination process via transient ZnP-trimer$^{\bullet+}$-$C_{60}^{\bullet-}$ is unlikely to proceed.[33a] This leaves electron tunneling via superexchange as the only operative mode. This picture is in sound agreement with the thermodynamic barrier that must be overcome in the formation of transient ZnP-trimer$^{\bullet+}$-$C_{60}^{\bullet-}$. At higher temperatures (> 300 K) the strong temperature dependence suggests thermally activated charge recombination.[33b] The activation barrier E_a, derived from the slope (0.2 eV), confirms the energy gap. Relative to our previous observation on exTTF-trimer-C_{60},[5] with an experimentally determined activation barrier of 0.5 eV, the smaller energy gap in **13a** reflects the lower HOMO of ZnP relative to exTTF.

In principle, electron and hole transfer may both contribute to charge recombination. Figure 14 shows that large LUMO (C_{60})–LUMO (wire) gaps of at least 1.1 eV result exclusively in an electron tunneling mechanism. Hole transfer from the HOMO at C_{60} to the HOMO at ZnP, on the other hand, may proceed via superexchange or hopping. In fact, the temperature dependence helps to recognize the interplay between the two processes. Once the hopping mechanism dominates and the hole migrates first to the wire, good HOMO (C_{60})–HOMO (wire) energy matching and strong electronic coupling leads to a kinetically fast and spectroscopically unresolvable recovery of the ground state.

Interestingly, the $ZnP^{\bullet+}/C_{60}^{\bullet-}$ pair in **13b** reveals a contrasting trend: charge recombination becomes slower with increasing temperature. We believe that decoupling of the

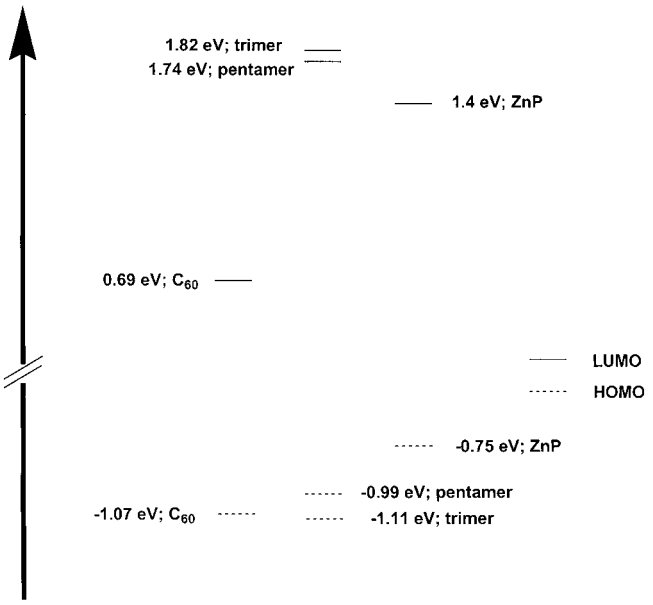

Figure 14. HOMO–LUMO levels, determined analogously to ref. [4a].

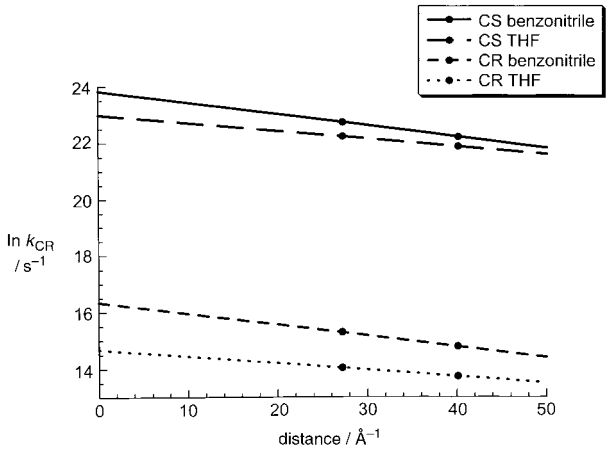

Figure 15. Dependence of electron-transfer rate constants on center-to-center distances for **13a** and **13b** in nitrogen-saturated THF (dashed line) and benzonitrile (solid line) at room temperature.

$ZnP^{\bullet+}/C_{60}^{\bullet-}$ pair by affecting the orbital alignment in the oPPV bridge is likely to be responsible for this.[34]

Following up on these temperature-induced changes, we consider the theoretically calculated geometries of **13a**/**13b** (Figure 2). The aryl groups of the tetraphenylporphyrin (TPP) moiety are in an orthogonal disposition relative to the mean plane of the porphyrin ring. Dihedral angles of around 66° are in agreement with those of other related TPP derivatives.[35] The TPP phenyl group that is linked to the oligomeric spacer also preserves a dihedral angle with the porphyrin ring of around 67°. In addition, we note the following trends. First, the TPP phenyl rings are not coplanar with the oligomeric part. Dihedral angles between the TPP phenyl ring and the first ring of the oligomer unit are about 30°.[36] Second, a deviation from planarity along the oligomer unit is noted. Relative to the phenyl rings at the other terminus of the oligomer, this deviation is much stronger for **13b** (63.7°) than for **13a** (55.3°).

These differences in geometry alone might not influence the charge-recombination mechanism, but they do help to rationalize why the reactivity of **13b** is so susceptible to temperature variation. More work is clearly needed to fully understand this interesting and unprecedented phenomenon.

Finally, plotting the electron transfer rates as a function of donor–acceptor separation (Figure 15) led to dependencies from which we determined attenuation factors β of 0.03 ± 0.005 Å^{-1}. The underlying wirelike behavior in **13a**/**13b** can be best understood in terms of π conjugation between the phenyl group of the donor/the oligophenylenevinylene bridge, and the pyrrolidine ring of the fullerene derivative. Values of 0.03 ± 0.005 Å^{-1} are exceptionally small relative to conjugated phenylenes,[37] but somewhat larger than those found in wires that carry exTTF (exTTF: 9,10-bis(1,3-dithiol-2-ylidene)-9,10-dihydroanthracene) as the electron donor.[5] Besides the different nature of the electron donor, the important difference between the previously reported exTTF-wire-C_{60} and the present ZnP-wire-C_{60} systems is the paraconjugation between the exTTF donor unit and the π-conjugated oligomer.

Conclusion

We have developed a multistep synthetic procedure for novel photo- and electroactive arrays, in which a zinc tetraphenylporphyrin donor is covalently linked to an electron-accepting fullerene through π-conjugated *p*-phenylenevinylene oligomers of variable length (trimer and pentamer).

A small attenuation factor β of 0.03 ± 0.005 Å^{-1} supports the notion of wirelike behavior in **13a**/**13b**. Important for the wirelike behavior is that the energies of the C_{60} HOMOs match those of the oPPVs. This facilitates electron/hole injection into the wire. Equally important is the strong electronic coupling, realized through the paraconjugation of the oPPVs. This leads to donor–acceptor coupling constants V of about 2.0 cm^{-1} and assists charge transfer reactions that exhibit a weak dependence on distance.

Experimental Section

General: FTIR spectra were recorded as KBr pellets on a Nicolet-Magna-IR 5550 spectrometer. Mass spectra with electrospray ionization (ESI) were recorded on a HP1100MSD spectrometer. UV/Vis spectra were recorded in dichloromethane solutions in 1 cm quartz cuvettes on a Varian Cary 50 Scan spectrophotometer. NMR spectra were recorded on Bruker AC-200 (^{1}H: 200 MHz; ^{13}C: 50 MHz), Bruker AC-300, or Varian XL-300 (^{1}H: 300 MHz; ^{13}C: 75 MHz) and Bruker DRX-500 or AMX-500 (^{1}H: 500 MHz; ^{13}C: 125 MHz) spectrometers at 298 K with partially deuterated solvents as internal standards. Chemical shifts are given as δ values (internal standard: TMS). π-Conjugated oligomers **8** and **11**,[16] porphyrins **2**[14] and **3**, **4**[15] were obtained by following previously described synthetic procedures. Elemental analyses were performed on

Perkin-Elmer 2400 CHN and 2400 CHNS/O analysers. Tetrahydrofuran was dried with sodium.

Cyclic voltammograms were recorded on a potentiostat/galvanostat AUTOLAB with PGSTAT30 equipped with software GPES for Windows version 4.8 in a conventional three-compartment cell by using a glassy carbon working electrode, a standard calomel reference electrode, Bu_4NClO_4 as supporting electrolyte, a *o*-dichlorobenzene/acetonitrile solvent mixture (4/1), and a scan rate of 200 $mV\,s^{-1}$.

Picosecond laser flash photolysis was carried out with 355 or 532 nm laser pulses from a mode-locked, Q-switched Quantel YG-501 DP Nd:YAG laser system (18 ps pulse width, 2–3 mJ per pulse). Nanosecond laser flash photolysis was performed with 355 or 532 nm laser pulses from a Quanta-Ray CDR Nd:YAG system (6 ns pulse width) in a front face excitation geometry.

Fluorescence lifetimes were measured with a Laser Strobe Fluorescence Lifetime Spectrometer (Photon Technology International) with 337 nm laser pulses from a nitrogen laser fiber-coupled to a lens-based T-formal sample compartment equipped with a stroboscopic detector. Details of the Laser Strobe systems are described on the manufacture's web site, http://www.pti-nj.com. Error limits of 10% must be considered.

Emission spectra were recorded with a SLM 8100 Spectrofluorometer. The experiments were performed at room temperature. Each spectrum represents an average of at least five individual scans, and appropriate corrections were applied whenever necessary.

5: A mixture of Zn^{II} bromomethyl porphyrinate **4** (0.2 g, 0.08 mmol) and $P(OCH_3)_3$ (3 mL) was refluxed for 2 h. The remaining trimethyl phosphite was distilled off and the residue was washed with hexane and methanol to give 0.2 g (97%) of porphyrin **5**. ^{1}H NMR (200 MHz, $CDCl_3$, 25 °C, TMS): $\delta = 9.03$ (s, 4H; $H_{pyrrolic}$), 8.98 (d, 2H, $^3J(H,H) = 4.7$ Hz; $H_{pyrrolic}$), 8.75 (d, 2H, $^3J(H,H) = 4.7$ Hz; $H_{pyrrolic}$), 8.1 (brs, 6H; H_{Ar}), 7.98 (d, 2H, $^3J(H,H) = 7.9$ Hz; H_{Ar}), 7.8 (brs, 3H; H_{Ar}), 6.67 (d, 2H, $^3J(H,H) = 7.9$ Hz; H_{Ar}), 2.71 (d, 6H, $^3J(H,P) = 11.0$ Hz; $POCH_3$), 2.62 (d, 2H, $^3J(H,P) = 20.0$ Hz; PCH_2); 1.53 ppm (s, 54H; $C(CH_3)_3$); ^{13}C NMR (75 MHz, $CDCl_3$, 25 °C, TMS): $\delta = 150.30$, 150.25, 150.10, 148.35, 142.59, 131.87, 129.94, 121.79, 120.42, 142.52, 132.06, 131.86, 131.81, 129.82, 129.91, 129.88, 61.23, 35.04, 31.80 ppm; IR (KBr) $\tilde{\nu} = 2960$, 2905, 2866, 1591, 1473, 1458, 1361, 1001, 798 cm^{-1}; UV/Vis (CH_2Cl_2): λ_{max} (ε) = 423 (407500), 552 (15500), 592 nm (6000 $mol^{-1}\,cm^3\,dm^{-1}$); MS (ESI): *m/z* (%): 1138 (100) [M^++H]; elemental analysis (%) calcd for $C_{71}H_{83}N_4O_3PZn{\cdot}H_2O$ (1154.83): C 73.29, H 7.58, N 4.95; found: C 73.05, H 7.76, N 4.63.

11a and **11b**: DIBAL-H (1 mL, 1 M in CH_2Cl_2, 1 mmol) was added to a refluxing solution of **10** (350 mg, 0.48 mmol) in dry methylene dichloride (25 mL) under argon. After 4 h of stirring the reaction was left to reach room temperature, and MeOH and a few drops of HCl were added with vigorous stirring. The phases were separated, and the aqueous phase was extracted with $CHCl_3$ (three times). The combined organic layers were washed with water and dried over $MgSO_4$. After evaporation of the solvent, the resulting solid was purified by careful flash chromatography on silica gel with a hexane/CH_2Cl_2 (1/4) as eluent to give first monoaldehyde **11b** (40 mg, 12%) and then **11a** (184 mg, 54%) as dark orange solids. Unconverted oligomer was also recovered.

11a: ^{1}H NMR (200 MHz, $CDCl_3$, 25 °C, TMS): $\delta = 10.0$ (s, 2H; CHO), 7.88 (d, 4H, $^3J(H,H) = 8.0$ Hz; H_{Ar}), 7.67 (d, 4H, $^3J(H,H) = 8.0$ Hz; H_{Ar}), 7.55 (brs, 8H; H_{Ar}), 7.54 (d, 2H, $^3J(H,H) = 16.4$ Hz; H_{olef}), 7.29 (d, 2H, $^3J(H,H) = 16.4$ Hz; H_{olef}), 7.15 (d, 4H, $^3J(H,H) = 16.4$ Hz; H_{olef}), 7.14 (s, 2H; H_{Ar}), 4.01 (t, 4H, $^3J(H,H) = 6.4$ Hz; CH_2O), 1.90 (m, 4H; CH_2), 1.58–1.18 (m, 12H; CH_2), 0.91 ppm (t, 6H; CH_3); ^{13}C NMR (50 MHz, $CDCl_3$, 25 °C, TMS): $\delta = 191.5$, 151.2, 143.5, 138.3, 135.3, 130.2, 127.3, 126.9, 126.8, 116.9, 109.0, 70.2, 31.6, 29.5, 26.0, 22.7, 14.0 ppm; IR (KBr): $\tilde{\nu} = 2923$, 2854, 1697, 1589, 1205, 1164, 960, 534 cm^{-1}; UV/Vis (CH_2Cl_2): λ_{max} (ε) = 324 (sh, 22400), 360 (34700), 438 nm (69100 $mol^{-1}\,cm^3\,dm^{-1}$); MS (ESI): *m/z* (%): 765 (15) [M^++Na], 722 (100), 638 (10), 304 (10); elemental analysis calcd (%) for $C_{52}H_{54}O_4$: C 84.06, H 7.30; found: C 83.78, H 7.68.

11b: ^{1}H NMR (200 MHz, $CDCl_3$, 25 °C, TMS): $\delta = 10.00$ (s, 1H; CHO), 7.88 (d, 2H, $^3J(H,H) = 8.0$ Hz; H_{Ar}), 7.68–7.61 (m, 6H, $H_{Ar\text{-}Olig}$), 7.55 (m, 8H; H_{Ar}), 7.54 (d, 2H, $^3J(H,H) = 16.3$ Hz; H_{olef}), 7.28 (d, 1H, $^3J(H,H) = 16.1$ Hz; H_{olef}), 7.23 (d, 1H, $^3J(H,H) = 16.1$ Hz; H_{olef}), 7.19 (s, 1H; H_{Ar}), 7.15 (d, 2H, $^3J(H,H) = 16.3$ Hz; H_{olef}), 7.14 (s, 1H; H_{Ar}), 7.09 (d, 1H, $^3J(H,H) = 16.3$ Hz; H_{olef}), 4.08 (t, 4H, $^3J(H,H) = 6.6$ Hz; CH_2O), 1.90 (q, 4H, $^3J(H,H) = 6.6$ Hz; CH_2), 1.56–1.25 (m, 12H; CH_2), 0.94 ppm (m, 6H; CH_3); ^{13}C NMR (50 MHz, $CDCl_3$, 25 °C, TMS): $\delta = 191.53$, 169.91, 151.24, 143.50, 141.92, 138.45, 138.29, 135.67, 135.38, 135.31, 132.49, 131.85, 130.25, 128.19, 127.28, 126.95, 126.87, 126.81, 126.35, 124.00, 110.64, 69.60, 31.64, 29.48, 25.97, 22.66, 14.05 ppm; IR (KBr) $\tilde{\nu} = 2923$, 2854, 2225, 1699, 1589, 1203, 1164, 962, 576 cm^{-1}; MS (ESI): *m/z* (%): 739 (100) [M^+].

General procedure for the preparation of dyads 12a,b: Potassium *tert*-butoxide (16 mg, 0.14 mmol) was slowly added to a refluxing solution of porphyrin **5** (0.10 mmol) and the corresponding oligomer **8** or **11** (0.20 mmol) in dry THF (10 mL) under argon. After 16 h, the crude mixture was cooled to room temperature and H_2O/CH_3OH (1/1) was added. The phases were separated and the aqueous phase was extracted with $CHCl_3$. The combined organic phases were washed with water and dried over $MgSO_4$. After evaporation of the solvent, the mixture was purified by chromatography on silica gel with hexane/toluene (1/3) as eluent to give the corresponding dyad. Unconverted oligomer was recovered in both cases.

ZnP-oPPV(3) (12a): Yield: 48%. ^{1}H NMR (500 MHz, $CDCl_3$, 25 °C, TMS): $\delta = 10.00$ (s, 1H; CHO), 9.0–8.9 (m, 8H; $H_{pyrrolic}$), 8.25 (d, 2H, $^3J(H,H) = 7.8$ Hz; $H_{Ar\text{-}Por}$), 8.1 (m, 6H; $H_{Ar\text{-}Por}$), 7.92 (d, 2H, $^3J(H,H) = 7.8$ Hz; $H_{Ar\text{-}Por}$), 7.88 (d, 2H, $^3J(H,H) = 8.1$ Hz; $H_{Ar\text{-}Olig}$), 7.81 (s, 3H; $H_{Ar\text{-}Porf}$), 7.68 (m, 4H; $H_{Ar\text{-}Olig}$), 7.62 (d, 2H, $^3J(H,H) = 8.1$ Hz; $H_{Ar\text{-}Olig}$), 7.56 (d, 2H, $^3J(H,H) = 16.4$ Hz; H_{olef}), 7.49 (d, 1H, $^3J(H,H) = 16.4$ Hz; H_{olef}), 7.44 (d, 1H, $^3J(H,H) = 16.4$ Hz; H_{olef}), 7.22 (d, 2H, $^3J(H,H) = 16.4$ Hz; H_{olef}), 7.2 (m, 2H; $H_{Ar\text{-}Olig}$), 4.1 (m, 4H; CH_2O), 1.9 (m, 4H; CH_2), 1.6–1.2 (m, 66H; CH_2), 0.97 ppm (m, 6H; CH_3); ^{13}C NMR (125 MHz, $CDCl_3$, 25 °C, TMS): $\delta = 191.64$, 151.53, 151.11, 150.54, 150.39, 150.00, 148.68, 148.53, 144.20, 141.81, 137.38, 135.10, 134.83, 132.31, 132.24, 131.61, 130.26, 130.01, 129.68, 129.59, 129.58, 128.99, 128.85, 128.45, 127.32, 127.03, 126.84, 125.96, 124.72, 123.30, 122.48, 122.47, 120.97, 120.78, 110.90, 110.47, 69.64, 69.53, 35.03, 31.75, 29.70, 29.44, 25.99, 22.68, 14.07 ppm; IR (KBr): $\tilde{\nu} = 2958$, 2930, 2862, 1699, 1593, 1492, 1475, 1422, 1362, 1247, 1208, 1164, 1001, 965, 799, 717 cm^{-1}; UV/Vis (CH_2Cl_2): λ_{max} (ε) = 249 (12900), 356 (19100), 403 (39800 sh), 424 (263000), 515 (4500), 551 (11700), 591 (4600), 650 nm (1300 $mol^{-1}\,cm^3\,dm^{-1}$); MS (ESI): *m/z* (%): 1549 (100) [M^+]; elemental analysis calcd (%) for $C_{105}H_{118}N_4O_3Zn{\cdot}2H_2O$ (1585.5): C 79.54, H 7.76, N 3.53; found: C 79.21, H 7.82, N 3.35.

ZnP-oPPV(5) (12b): Yield: 42%. ^{1}H NMR (200 MHz, $CDCl_3$, 25 °C, TMS): $\delta = 9.90$ (s, 1H; CHO), 9.03 (s, 8H; $H_{pyrrolic}$), 8.25 (d, 2H, $^3J(H,H) = 8.0$ Hz; $H_{Ar\text{-}Por}$), 8.1 (brs, 6H; $H_{Ar\text{-}Por}$), 7.89 (d, 2H, $^3J(H,H) = 8.0$ Hz; $H_{Ar\text{-}Por}$), 7.8 (brs, 3H; $H_{Ar\text{-}Por}$), 7.6–7.4 (m, 14H; $H_{Ar\text{-}Olig}$), 7.59 (d, 6H, $^3J(H,H) = 16.3$ Hz; H_{olef}), 7.2–7.0 (m, 4H; $H_{Ar\text{-}Olig}$), 7.14 (d, 6H, $^3J(H,H) = 16.3$ Hz; H_{olef}), 4.0 (m, 4H; CH_2O), 1.9 (m, 4H; CH_2), 1.5–1.2 (m, 66H; CH_2), 0.9 ppm (m, 6H; CH_3); ^{13}C NMR (75 MHz, $CDCl_3$), 25 °C, TMS): $\delta = 191.57$, 151.08, 150.40, 150.34, 149.95, 148.49, 143.44, 142.48, 141.83, 138.28, 137.36, 136.85, 136.79, 136.52, 136.34, 135.55, 135.14, 134.85, 132.30, 132.15, 131.82, 131.60, 130.87, 130.12, 129.69, 129.61, 129.01, 128.78, 128.29, 128.04, 127.26, 127.01, 126.87, 124.72, 123.94, 123.33, 122.54, 122.42, 120.73, 120.30, 110.52, 69.54, 35.02, 31.91, 31.74, 31.64, 31.42, 29.69, 29.54, 22.68, 14.12 ppm; IR (KBr): $\tilde{\nu} = 2953$, 2923, 2853, 1697, 1592, 1464, 1422, 1362, 1247, 1204, 1165, 1000, 961, 821, 797, 717 cm^{-1}; UV/Vis (CH_2Cl_2): λ_{max} (ε) = 245 (49000), 357 (49000), 425 (371500), 551 (20000), 591 nm (8500 $mol^{-1}\,cm^3\,dm^{-1}$). MS (ESI): *m/z* (%): 1753 (100) [M^+]; elemental analysis (%) calcd for $C_{121}H_{130}N_4O_3Zn$ (1753.8): C 82.87, H 7.47, N 3.19; found: C 83.12, H 7.30, N 3.29.

General procedure for the preparation of triads 13a,b: A mixture of the corresponding dyad **12a** or **12b** (0.04 mmol), [60]fullerene (0.04 mmol), and *N*-methylglycine (0.12 mmol) in 25 mL of chlorobenzene was refluxed for 24 h. After cooling to room temperature, the crude mixture was purified by column chromatography on silica gel with CS_2 to elute the unconverted fullerene followed by hexane/toluene (2/3) (**13a**) or hexane/THF (3/1) (for **13b**) to yield the corresponding triad.

ZnP-oPPV(3)-C_{60} (13a): Yield: 51% ^{1}H NMR (200 MHz, $CDCl_3$, 25°C, TMS): δ = 8.96 (s, 8H; $H_{pyrrolic}$), 8.19 (d, 2H, ^3J(H,H) = 6.5 Hz; $H_{Ar\text{-}Porf}$), 8.1 (br s, 6H; $H_{Ar\text{-}Porf}$), 7.89 (d, 2H, ^3J(H,H) = 6.5 Hz; $H_{Ar\text{-}Porf}$), 7.8 (br s, 3H; $H_{Ar\text{-}Porf}$), 7.7–7.4 (m, 12H; $H_{Ar\text{-}Olig}$, H_{olef}), 7.2–7.1 (m, 4H; H_{olef}); 4.77 (d, 1H, ^2J(H,H) = 8.8 Hz; $H_{pyrrolidine}$), 4.70 (s, 1H; $H_{pyrrolidine}$), 4.0 (m, 5H; CH_2O, $H_{pyrrolidine}$), 2.79 (s, 3H; CH_3N), 1.9 (m, 4H; CH_2), 1.7–1.4 (m, 66H; CH_2), 0.9 ppm (m, 6H; CH_3); ^{13}C NMR (75 MHz, $CDCl_3/CS_2$), 25°C, TMS): δ = 155.72, 155.69,153.50, 153.27, 152.95, 152.80, 152.70, 150.88, 150.80, 150.13, 149.73, 148.16, 146.66, 146.13, 145.85, 145.73, 145.51, 145.35, 145.29, 145.15, 144.97, 144.83, 144.73, 144.57, 144.47, 144.42, 144.24, 144.11, 144.08, 143.91, 143.87, 143.77, 142.74, 142.45, 142.21, 142.12, 141.96, 141.86, 141.74, 141.48, 141.18, 141.01, 139.53, 139.28, 139.13, 137.98, 137.27, 136.35, 136.28, 135.90, 135.74, 135.01, 134.79, 132.18, 132.02, 131.81, 131.53, 129.64, 129.51, 129.39, 129.22, 128.74, 128.14, 128.08, 127.92, 126.81, 126.62, 126.45, 124.63, 123.80, 123.21, 122.27, 122.19, 120.61, 120.19, 110.12, 109.94, 83.14, 83.06, 69.13, 69.07, 39.80, 34.73, 31.63, 29.81, 29.56, 26.06, 22.88, 14.21 ppm; IR (KBr): $\tilde{\nu}$ = 2950, 2926, 2857, 1590, 1463, 1421, 1204, 1180, 1068, 1001, 797, 716, 527 cm^{-1}; UV/Vis (CH_2Cl_2): λ_{max} (ε) = 255 (129000), 329 (61500), 403 (59000 sh), 424 (457000), 513 (7000), 550 (24000), 590 nm (9500 mol^{-1}cm^{3}dm^{-1}); MS (ESI): *m/z* (%): 2297 (100) [M^+]; elemental analysis (%) calcd for $C_{167}H_{123}N_5O_2Zn{\cdot}4H_2O$: C 84.66, H 5.57, N 2.96; found: C 84.23, H 5.67, N, 2.99.

ZnP-oPPV(5)-C_{60} (13b): Yield: 32% ^{1}H NMR (200 MHz, $CDCl_3$, 25°C, TMS): δ = 8.97 (s, 8H; $H_{pyrrolic}$), 8.18 (d, 2H, ^{3}J(H,H) = 7.4 Hz; $H_{Ar\text{-}Porf}$), 8.1 (br s, 6H; $H_{Ar\text{-}Porf}$), 7.89 (d, 2H, ^{3}J(H,H) = 7.4 Hz; $H_{Ar\text{-}Porf}$), 7.8 (br s, 3H; $H_{Ar\text{-}Porf}$), 7.6–7.4 (m, 20H; $H_{Ar\text{-}Olig}$, H_{olef}), 7.1–7.0 (m, 8H; H_{olef}); 4.69 (d, 1H, ^{2}J(H,H) = 7.9 Hz; $H_{pyrrolidine}$), 4.58 (s, 1H; $H_{pyrrolidine}$), 4.0 (m, 4H; CH_2O), 3.93 (d, 1H, ^{3}J(H,H) = 7.9 Hz; $H_{pyrrolidine}$), 2.75 (s, 3H; CH_3N), 1.9 (m, 4H; CH_2), 1.7–1.3 (m, 66H; CH_2), 1.0 ppm (m, 6H; CH_3); ^{13}C NMR (125 MHz, $CDCl_3/CS_2$), 25°C, TMS): δ = 155.73, 155.38, 153.10, 152.91, 152.59, 150.88, 150.57, 150.16, 149.74, 148.21, 146.58, 145.84, 145.53, 145.41, 145.24, 144.54, 144.45, 143.87, 143.68, 143.32, 142.31, 141.79, 141.29, 140.89, 139.37, 139.01, 137.37, 137.18, 137.01, 136.74, 136.52, 136.26, 136.11, 136.03, 135.69, 135.17, 134.85, 132.21, 132.11, 132.03, 131.53, 130.01, 129.67, 129.50, 129.01, 128.74, 128.55, 128.18, 128.01, 127.80, 127.72, 127.48, 127.38, 126.94, 126.86, 126.75, 126.25, 126.12, 125.02, 124.66, 123.96, 123.38, 123.24, 122.30, 122.22, 121.95, 120.63, 120.19, 110.09, 110.02, 82.89, 69.54, 69.13, 39.74, 34.76, 32.01, 31.77, 31.66, 31.33, 29.82, 29.57, 26.06, 22.87, 14.19 ppm; IR (KBr): $\tilde{\nu}$ = 2962, 2876, 1694, 1595, 1474, 1384, 1260, 1093, 1017, 798, 623, 527 cm^{-1}; UV/Vis (CH_2Cl_2): λ_{max} (ε) = 254 (72500), 330 (41500), 405 (53500 sh), 425 (234500), 513 (6500), 551 (13500), 591 nm (7000 mol^{-1}cm^{3}dm^{-1}); MS (ESI): *m/z* (%): 2501 (100) [M^+]; elemental analysis (%) calcd for $C_{183}H_{135}N_5O_2Zn{\cdot}CH_3OH$ (2533.5): C 87.23, H 5.53, N 2.76; found: C 87.26, H 5.61, N 2.71.

15: Potassium *tert*-butoxide (168 mg; 1.5 mmol) was added portionwise to a solution of **6** (1.05 g; 2 mmol) in dry THF (130 mL) at room temperature. The reaction was stirred for 20 min, and then a solution of benzaldehyde (106 mg, 1.0 mmol) in dry THF (35 mL) was added dropwise. After 2 h, methanol (5 mL) was added to the reaction mixture and the solvent was evaporated. The resulting solid was purified by flash chromatography (silica gel, CH_2Cl_2, CH_2Cl_2/MeOH (98/2)) to obtain 265 mg (53%) of **15** as a pale yellow oil.

^{1}H NMR (200 MHz, $CDCl_3$, 25°C, TMS): δ = 7.54–7.49 (m, 2H; H_{Ar}), 7.39 (m, 1H; H_{Ar}), 7.35 (s, 1H; H_{Ar}), 7.34 (d, 1H, ^3J(H,H) = 16.4 Hz; H_{olef}), 7.08 (d, 1H, ^3J(H,H) = 16.4 Hz; H_{olef}), 7.07 (s, 1H; H_{Ar}), 6.92 (d, 1H, ^3J(H,H) = 2.8 Hz; H_{Ar}), 6.88 (d, 1H, ^3J(H,H) = 1.3 Hz; H_{Ar}), 3.97 (m, 4H; CH_2O), 3.68 (d, 6H, ^3J (H,P) = 11.0 Hz; $POCH_3$), 3.26 (d, 2H, ^3J (H,P) = 21.0 Hz; PCH_2), 1.80 (m, 4H; CH_2), 1.53–1.25 (m, 12H; CH_2), 0.90 ppm (m, 6H; CH_3); ^{13}C NMR (75 MHz, $CDCl_3$, 25°C, TMS): δ = 150.93, 150.78, 137.94, 128.70, 128.66, 128.59, 127.34, 126.56, 126.46, 126.03, 123.66, 121.19, 120.37, 120.17, 69.52, 69.12, 52.79, 52.65, 31.61, 31.58, 29.38, 25.79, 22.61, 13.90 ppm; IR (KBr): $\tilde{\nu}$ = 2950, 2935, 2856, 1506, 1475, 1421, 1269, 1213, 1058, 1028, 871, 754 cm^{-1}; UV/Vis (CH_2Cl_2) λ_{max} (ε): 229 (6700), 295 (12900), 342 nm (9300 mol^{-1}cm^{3}dm^{-1}); MS (EI): *m/z* (%): 522 (29) [M^+], 418 (35) [$M^+ - C_6H_{13}$], 393 (3), 334 (89) [$M^+ - C_6H_{13}$], 302 (17), 223 (100), 91 (14), 86 (23).

16: Potassium *tert*-butoxide (45 mg, 0.40 mmol) was added portionwise to a solution of **15** (150 mg, 0.30 mmol) and **7** (63 mg, 0.30 mmol) in dry THF (20 mL), and the reaction mixture was stirred at room temperature for 40 min under argon. After removing the solvent, the residue was dissolved in $CHCl_3$ (100 mL), 1 M HCl (100 mL) added, and the reaction mixture stirred overnight. The organic phase was separated and dried over $MgSO_4$. Further purification was accomplished by flash chromatography on silica gel with hexane/CH_2Cl_2 (1/1) to obtain 110 mg (72%) of **16** as an orange solid.

^{1}H NMR (200 MHz, $CDCl_3$, 25°C, TMS): δ = 10.00 (s, 1H; CHO), 7.87 (d, 1H, ^{3}J(H,H) = 8.0 Hz; H_{Ar}), 7.66 (d, 1H, ^{3}J(H,H) = 8.3 Hz; H_{Ar}), 7.56 (d, 1H, ^{3}J(H,H) = 16.1 Hz; H_{olef}), 7.54 (d, 2H, ^{3}J(H,H) = 8.3 Hz; H_{Ar}), 7.49 (d, 1H, ^{3}J(H,H) = 16.3 Hz; H_{olef}), 7.39 (d, 1H, ^{3}J(H,H) = 7.5 Hz; H_{Ar}), 7.35 (d, 1H, ^{3}J(H,H) = 7.5 Hz; H_{Ar}), 7.26 (d, 1H, ^{3}J(H,H) = 16.1 Hz; H_{olef}), 7.16 (d, 1H, ^{3}J(H,H) = 16.1 Hz; H_{olef}), 7.14 (s, 1H; H_{Ar}), 7.13 (s, 1H; H_{Ar}), 4.07 (m, 4H; CH_2O), 1.89 (m, 4H; CH_2), 1.59–1.26 (m, 12H; CH_2), 0.93 ppm (t, 6H; CH_3); ^{13}C NMR (50 MHz, $CDCl_3$, 25°C, TMS): δ = 191.56, 151.53, 151.09, 144.21, 137.84, 135.19, 130.22, 129.39, 128.66, 128.05, 127.57, 127.30, 127.17, 126.82, 126.58, 125.92, 123.37, 110.98, 110.60, 69.67, 69.54, 31.62, 29.47, 29.44, 25.96, 22.64, 14.01 ppm; IR (KBr): $\tilde{\nu}$ = 2951, 2930, 2856, 1697, 1597, 1491, 1466, 1423, 1210, 1165, 964, 844, 810, 752, 690 cm^{-1}; UV/Vis (CH_2Cl_2): λ_{max} (ε) = 246 (15400), 336 (19000), 408 nm (25600 mol^{-1}cm^{3}dm^{-1}); MS (EI): *m/z* (%): 510 (100) [M^+], 418 (10) [$M^+ - C_6H_{13}$], 105 (8).

Dyads 17 and 18: These two reference compounds were prepared by following the same synthetic methodology used for triads **13a**,**b** with *N*-octylglycine[38] instead of *N*-methylglycine.

17: Yield 42%; ^{1}H NMR (200 MHz, $CDCl_3$, 25°C, TMS): δ = 7.79 (d, 2H, *J*(H,H) = 7.0 Hz; H_{Ar}), 7.60–7.32 (m, 7H; H_{Ar}), 7.20 (d, 1H, ^3J(H,H) = 16.1 Hz; H_{olef}), 7.15 (d, 1H, ^3J(H,H) = 16.1 Hz; H_{olef}), 7.12 (d, 2H, ^3J(H,H) = 16.1 Hz; H_{olef}), 7.10 (s, 1H; H_{Ar}), 5.11 (d, 1H, ^2J(H,H) = 10.0 Hz; $H_{pyrrolidine}$), 5.07 (s, 1H; $H_{pyrrolidine}$), 4.13 (d, 1H, ^2J(H,H) = 10.0 Hz; $H_{pyrrolidine}$), 4.03 (m, 4H; CH_2O), 3.28 (m, 1H; CH_2N), 2.58 (m, 1H; CH_2N), 1.86 (m, 6H; CH_2), 1.54–1.26 (m, 22H; CH_2), 0.91 ppm (m, 9H; CH_3); ^{13}C NMR (50 MHz, $CDCl_3$, 25°C, TMS): δ = 151.17, 151.10, 147.32, 146.48, 146.32, 146.26, 146.22, 146.15, 146.10, 145.95, 145.92, 145.79, 145.55, 145.50, 145.34, 145.32, 145.27, 145.24, 145.16, 144.73, 144.65, 144.40, 143.16, 142.99, 142.68, 142.58, 142.54, 142.34, 142.27, 142.16, 142.13, 142.08, 142.03, 141.94, 141.89, 141.67, 141.52, 140.18, 140.13, 139.88, 139.55, 138.09, 137.97, 135.77, 135.70, 129.82, 128.86, 128.62, 128.32, 127.40, 127.06, 126.79, 126.73, 126.52, 123.91, 123.53, 110.78, 110.64, 82.48, 69.61, 69.57, 68.91, 53.24, 31.94, 31.62, 29.65, 29.47, 29.34, 27.58, 25.93, 22.72, 22.65, 22.63, 14.16, 14.06, 14.01 ppm; IR (KBr): $\tilde{\nu}$ = 2920, 2850, 1595, 1508, 1491, 1460, 1419, 1257, 1188, 1016, 960, 527 cm^{-1}; UV/Vis (CH_2Cl_2): λ_{max} (ε) = 246 (115400), 255 (123600), 328 (64600), 394 nm (54400 mol^{-1}cm^{3}dm^{-1}); MS (ESI): m/z (%): 1356 (100) [M^+].

18: Yield 49%; ^{1}H NMR (200 MHz, $CDCl_3$, 25°C, TMS): δ = 7.80 (m, 2H; H_{Ar}), 7.64 (d, 2H, ^3J(H,H) = 8.6 Hz; H_{Ar}), 7.58 (d, 2H, ^3J(H,H) = 8.6 Hz; H_{Ar}), 7.56 (d, 2H, ^3J(H,H) = 8.6 Hz; H_{Ar}), 7.53 (m, 4H), 7.52 (d, 2H, ^3J(H,H) = 16.3 Hz; H_{olef}), 7.48 (m, 4H; H_{Ar}), 7.22 (d, 2H, ^3J(H,H) = 16.3 Hz; H_{olef}), 7.14 (d, 2H, ^3J(H,H) = 16.3 Hz; H_{olef}), 7.12 (s, 2H; H_{Ar}), 7.09 (d, 2H, ^3J(H,H) = 16.3 Hz; H_{olef}), 5.10 (d, 1H, ^2J(H,H) = 9.6 Hz; $H_{pyrrolidine}$), 5.06 (s, 1H; $H_{pyrrolidine}$), 4.11 (d, 1H, ^2J(H,H) = 9.6 Hz; $H_{pyrrolidine}$), 4.06 (m, 4H; CH_2O), 3.24 (m, 1H; CH_2N), 2.57 (m, 1H; CH_2N), 1.88 (m, 6H; CH_2), 1.56 (m, 8H; CH_2), 1.40–1.26 (m, 14H; CH_2), 0.93 ppm (m, 9H; CH_3); ^{13}C NMR (75 MHz, CDCl3, 25°C, TMS): δ = 156.60, 154.28, 153.58, 153.54, 151.21, 151.13, 147.28, 146.81, 146.49, 146.28, 146.23, 146.19, 146.14, 146.10, 146.07, 145.91, 145.75, 145.53, 145.47, 145.30, 145.24, 145.20, 145.11, 144.70, 144.60, 144.37, 143.13, 142.97, 142.66, 142.55, 142.33, 142.26, 142.08, 141.99, 141.90, 141.82, 141.65, 141.50, 140.15, 140.11, 139.86, 139.50, 138.45, 137.40, 137.36, 136.88, 136.84, 136.55, 136.42, 135.82, 135.69, 135.30, 132.47, 132.05, 129.82, 128.66, 128.48, 128.03, 127.28, 127.17, 126.93, 126.85, 126.79, 126.67, 126.29, 124.12, 123.40, 119.05, 110.61, 110.51, 110.43, 82.36, 69.57, 69.52, 68.97, 66.87, 53.17, 31.96, 31.63, 29.67, 29.46, 29.36, 28.36, 27.58, 25.96, 22.74, 22.65, 14.19, 14.05 ppm; IR (KBr): $\tilde{\nu}$ = 2922, 2852, 2222, 1630, 1593, 1508, 1491, 1464, 1421, 1203, 1172, 1018, 960, 527 cm^{-1}; UV/Vis (CH_2Cl_2): λ_{max}

(ε) = 245 (111500), 255 (119300), 308 (54500), 349 (59800), 431 nm (74000 $mol^{-1} cm^3 dm^{-1}$); MS (ESI): *m/z* (%): 1585 (100) [M^+–H].

Acknowledgement

Financial support from the MCYT of Spain (Project BQU2002-00855). Part of this work was supported by the Office of Basic Energy Sciences of the U.S. Department of Energy (Contribution No. NDRL-4577 from the Notre Dame Radiation Laboratory). We thank Jeff Ramey for doing some of the photophysical experiments.

[1] a) *An Introduction to Molecular Electronics* (Eds.: M. C. Petty, M. R. Bryce, D. Bloor), Oxford University Press, New York, **1995**; b) *Molecular Electronics* (Eds.: J. Jortner, M. Ratner), Blackwell, Oxford, **1997**; c) M. A. Fox, *Acc. Chem. Res.* **1999**, *32*, 201–207. For a recent review on molecular electronics, see: d) R. L. Carroll, C. B. Gorman, *Angew. Chem.* **2002**, *114*, 4556–4579; *Angew. Chem. Int. Ed.* **2002**, *41*, 4378–4400.

[2] a) H. M. McConnell, *J. Phys. Chem.* **1961**, *65*, 508–515; b) P. F. Barbara, T. J. Meyer, M. A. Ratner, *J. Phys. Chem.* **1996**, *100*, 13148–13168; c) N. Robertson, C. A. McGowan, *Chem. Soc. Rev.* **2003**, *32*, 96–103.

[3] a) M. D. Ward, *Chem. Soc. Rev.* **1995**, *24*, 121–134; b) J. M. Tour, *Chem. Rev.* **1996**, *96*, 537–553; c) P. F. H. Schwab, M. D. Levin, J. Michl, *Chem. Rev.* **1999**, *99*, 1863–1933; d) R. E. Martin, T. Mäder, F. Diederich, *Angew. Chem.* **1999**, *111*, 834–838; *Angew. Chem. Int. Ed.* **1999**, *38*, 817–821. For a recent review on functionalized oligomers, see: e) J. L. Segura, N. Martín, *J. Mater. Chem.* **2000**, *10*, 2403–2435; f) J. M. Tour, *Acc. Chem. Res.* **2000**, *33*, 791–804 .

[4] a) W. B. Davis, W. A. Svec, M. A. Ratner, M. R. Wasielewski, *Nature* **1998**, *396*, 60–63; b) G. Pourtis, D. Beljonne, J. Cornil, M. A. Ratner, J. L. Brédas, *J. Am. Chem. Soc.* **2002**, *124*, 4436–4447.

[5] F. Giacalone, J. L. Segura, N. Martín, D. M. Guldi, *J. Am. Chem. Soc.* **2004**, *126*, 5340–5341.

[6] For a recent review on porphyrins as precursors for molecular devices, see: D. Holten, D. F. Bocian, J. S. Lindsey, *Acc. Chem. Res.* **2002**, *35*, 57–69.

[7] a) H. Imahori, K. Hagiwara, T. Akiyama, M. Aoki, S. Taniguchi, T. Okada, M. Shirakawa, Y. Sakata, *Chem. Phys. Lett.* **1996**, *263*, 545–550; b) D. M. Guldi, K.-D. Asmus, *J. Am. Chem. Soc.* **1997**, *119*, 5744–5745; c) N. V. Tkachenko, C. Guenther, H. Imahori, K. Tamaki, Y. Sakata, S. Fukuzumi, H. Lemmetyinen, *Chem. Phys. Lett.* **2000**, *326*, 344–350; d) H. Imahori, K. Tamaki, H. Yamada, K. Yamada, Y. Sakata, Y. Nishimura, I. Yamazaki, M. Fujitsuka, O. Ito, *Carbon* **2000**, *38*, 1599–1605; e) H. Imahori, N. V. Tkachenko, V. Vehmanen, K. Tamaki, H. Lemmetyinen, Y. Sakata, S. J. Fukuzumi, *J. Phys. Chem. A* **2001**, *105*, 1750–1756.

[8] For some reviews, see: a) M. R. Wasielewski, in *Photoinduced Electron Transfer, Part A* (Eds.: M. A. Fox, M. Chanon), Elsevier, Amsterdam, **1988**, pp. 161–206; b) G. L. Closs, J. R. Miller, *Science* **1988**, *240*, 440–447; c) J. S. Connolly, J. R. Bolton in *Photoinduced Electron Transfer, Part D* (Eds. M.: A. Fox, M. Chanon), Elsevier, Amsterdam, **1988**, pp. 303–393; d) M. D. Newton, *Chem. Rev.* **1991**, *91*, 767–792; e) M. R. Wasielewski, *Chem. Rev.* **1992**, *92*, 435; f) D. Gust, T. A. Moore, A. L. Moore, *Acc. Chem. Res.* **1993**, *26*, 198–205; g) M. N. Paddon-Row, *Acc. Chem. Res.* **1994**, *27*, 18–25; h) H. Kurreck, M. Huber, *Angew. Chem.* **1995**, *107*, 929–947; *Angew. Chem. Int. Ed. Engl.* **1995**, *34*, 849–866; i) I. R. Gould, S. Farid, *Acc. Chem. Res.* **1996**, *29*, 522–528; j) V. Balzani, A. Juris, M. Venturi, S. Campagna, S. Serroni, *Chem. Rev.* **1996**, *96*, 759–833; k) I. Willner, *Acc. Chem. Res.* **1997**, *30*, 347–356; l) M. Bixon, J. Jortner in *Electron Transfer—From Isolated Molecules to Biomolecules, Part 1* (Eds.: M. Bixon, J. Jortner), Wiley, New York, **1999**, pp. 35–202; m) P. Piotrowiak, *Chem. Soc. Rev.* **1999**, *28*, 143–150; n) D. Gust, T. A. Moore, *The Porphyrin Handbook*, *Vol. 8* (Eds.: K. M. Kadish, K. M. Smith, R. Guilard), Academic Press, San Diego, CA, **2000**, pp. 153–190; o) P. J. Bracher, D. Schuster in *Fullerenes: From Synthesis to Optoelectronic Properties* (Eds.: D. M. Guldi, N. Martín), Kluwer Academic, Dordrech, **2002**, pp. 163–212.

[9] a) H. Imahori, Y. Sakata, *Adv. Mater.* **1997**, *9*, 537–546; b) M. Prato, *J. Mater. Chem.* **1997**, *7*, 1097; c) N. Martín, L. Sánchez, B. Illescas, I. Pérez, *Chem. Rev.* **1998**, *98*, 2527–2547; d) F. Diederich, M. Gomez-Lopez, *Chem. Soc. Rev.* **1999**, *28*, 263–277; e) H. Imahori, Y. Sakata, *Eur. J. Org. Chem.* **1999**, 2445–2457; f) D. M. Guldi, *Chem. Commun.* **2000**, 321–327; g) D. Gust, T. A. Moore, A. L. Moore, *Acc. Chem. Res.* **2001**, *34*, 40–48; h) D. M. Guldi, N. Martín, *J. Mater. Chem.* **2002**, *12*, 1978–1992.

[10] a) H. Imahori, K. Hagiwara, M. Aoki, T. Akiyama, S. Taniguchi, T. Okada, M. Shirakawa, Y. Sakata, *J. Am. Chem. Soc.* **1996**, *118*, 11771–11782; b) M. J. Shephard, M. N. Paddon-Row, *Aust. J. Chem.* **1996**, *49*, 395; c) P. A. Liddell, D. Kuciauskas, J. P. Sumida, B. Nash, D. Nguyen, A. L. Moore, T. A. Moore, D. Gust, *J. Am. Chem. Soc.* **1997**, *119*, 1400–1405; d) P. S. Baran, R. R. Monaco, A. U. Khan, D. I. Schuster, S. R. Wilson, *J. Am. Chem. Soc.* **1997**, *119*, 8363–8364; e) T. D. M. Bell, T. A. Smith, K. P. Ghiggino, M. G. Ranasinghe, M. J. Shephard, M. N. Paddon-Row, *Chem. Phys. Lett.* **1997**, *268*, 223–228; f) N. Armaroli, F. Diederich, C. O. Dietrich-Buchecker, L. Flamigni, G. Marconi, J.-F. Nierengarten, J.-P. Sauvage, *Chem. Eur. J.* **1998**, *4*, 406–416; g) J.-F. Nierengarten, C. Schall, J.-F. Nicoud, *Angew. Chem.* **1998**, *110*, 2037–2040; *Angew. Chem. Int. Ed.* **1998**, *37*, 1934–1936; h) D. I. Schuster, P. Cheng, S. R. Wilson, V. Prokhorenko, M. Katterle, A. R. Holzwarth, S. E. Braslavsky, G. Klihm, R. M. Williams, C. Luo, *J. Am. Chem. Soc.* **1999**, *121*, 11599–11600; i) N. V. Tkachenko, L. Rantala, A. Y. Tauber, J. Helaja, P. H. Hynninen, H. Lemmetyinen, *J. Am. Chem. Soc.* **1999**, *121*, 9378–9387; j) F. D′Souza, G. R. Deviprasad, M. S. Rahman, J.-P. Choi, *Inorg. Chem.* **1999**, *38*, 2157–2160; k) D. Kuciauskas, P. A. Liddell, S. Lin, T. E. Johnson, S. J. Weghorn, J. S. Lindsey, A. L. Moore, T. A. Moore, D. Gust, *J. Am. Chem. Soc.* **1999**, *121*, 8604–8614; l) N. V. Tkachenko, E. Vuorimaa, T. Kesti, A. S. Alekseev, A. Y. Tauber, P. H. Hynninen, H. Lemmetyinen, *J. Phys. Chem. B* **2000**, *104*, 6371–6379; m) F.-P. Montforts, O. Kutzki, *Angew. Chem.* **2000**, *112*, 612–614; *Angew. Chem. Int. Ed.* **2000**, *39*, 599–601; n) F. D′Souza, G. R. Deviprasad, M. E. El-Khouly, M. Fujitsuka, O. Ito, *J. Am. Chem. Soc.* **2001**, *123*, 5277–5284; o) S. Fukuzumi, K. Ohkubo, H. Imahori, J. Shao, Z. Ou, G. Zheng, Y. Chen, R. K. Pandey, M. Fujitsuka, O. Ito, K. M. Kadish, *J. Am. Chem. Soc.* **2001**, *123*, 10676–10683.

[11] A triad comprising porphyrin, oligothiophene, and fullerene components has been recently synthesized: a) J. Ikemoto, K. Takimiya, Y. Aso, T. Otsubo, M. Fujitsuka, O. Ito, *Org. Lett.* **2002**, *4*, 309–311; b) T. Otsubo, Y. Aso, K. Takimiya, *J. Mater. Chem.* **2002**, *12*, 2565–2575.

[12] J. S. Lindsey, K. A. MacCrum, J. S. Tyhonas, Y.-Y. Chuang, *J. Org. Chem.* **1994**, *59*, 579–587.

[13] M. S. Newman, L. F. Lee, *J. Org. Chem.* **1972**, *37*, 4468–4469.

[14] H. Tamiaki, S. Suzuki, K. Maruyama, *Bull. Chem. Soc. Jpn.* **1993**, *66*, 2633–2637.

[15] X. J. Salom-Roig, J.-C. Chambron, C. Goze, V. Heitz, J.-P. Sauvage, *Eur. J. Org. Chem.* **2002**, *67*, 3276–3280.

[16] These symmetric compounds (ZnP-oPPV-ZnP) can be prepared in larger amounts by controlling the stoichiometry of the reaction. The synthesis and characterization of these compounds will be reported elsewhere.

[17] a) M. Prato, M. Maggini, *Acc. Chem. Res.* **1998**, *31*, 519–526; b) N. Tagmatarchis, M. Prato, *Synlett* **2003**, 768–779.

[18] *Electronic Materials: The Oligomer Approach* (Eds.: K. Müllen, G. Wegner), Wiley-VCH, Weinheim, **1998**, Chapter 1.

[19] U. Stalmach, H. Kolshorn, I. Brehm, H. Meier, *Liebigs Ann.* **1996**, 1449–1456.

[20] Compound **11b** bearing one formyl group can be obtained as the major product from pentamer **10** by using DIBAL-H in a 1:1 stoichiometry.

[21] F. D'Souza, G. R. Deviprasad, M. E. Zandler, V. T. Hoang, A. Klykov, M. VanStipdonk, A. Perera, M. E. El-Khouly, M. Fujitsuka, O. Ito, *J. Phys. Chem. A* **2002**, *106*, 3243–3252.
[22] D. M. Guldi, C. Luo, M. Prato, A. Troisi, F. Zerbetto, M. Scheloske, E. Dietel, W. Bauer, A. Hirsch, *J. Am. Chem. Soc.* **2001**, *123*, 9166–9167.
[23] D. M. Guldi, M. Prato, *Acc. Chem. Res.* **2000**, *33*, 695–703.
[24] In line with such strong quenching, complementary fluorescence lifetime measurements did not yield any detectable signals for **12a** and **12b** in the 450–550 nm region that falls within the 100 ps detection limits. Note that the strong fluorescence of the oligomeric building blocks has lifetimes that are 1.2 and 0.8 ns for the **trimer** and **pentamer**, respectively.
[25] Both oligomeric building blocks have characteristic triplet–triplet absorptions (see previous section and Figure 5).
[26] Shifting the excitation from the 400–420 nm range to shorter wavelengths, where the C_{60} and oligomer absorptions increase and decrease, respectively, did not change the picture. The fluorescence quantum yields of both moieties remained constant, despite the stronger C_{60} contribution, which proves that the C_{60} fluorescence is stable.
[27] a) J. L. Segura, R. Gómez, N. Martín, C. Luo, D. M. Guldi, *Chem. Commun.* **2000**, 701–702; b) D. M. Guldi, C. Luo, A. Swartz, R. Gómez, J. L. Segura, N. Martín, C. Brabec, N. S. Sariciftci, *J. Org. Chem.* **2002**, *67*, 1141–1152.
[28] It is important that oligomer fluorescence quenching remained unaffected in the ZnP-trimer-C_{60} (**13a**) and ZnP-pentamer-C_{60} (**13b**) wires. We have to consider, however, competition between energy-transfer events, as supported by the investigations dealing with the ZnP-oligomer and oligomer-C_{60} precursor systems.
[29] a) R. A. Marcus, N. Sutin, *Biochim. Biophys. Acta* **1985**, *811*, 265–322; b) R. A. Marcus, *Angew. Chem.* **1993**, *105*, 1161–1172; *Angew. Chem. Int. Ed. Engl.* **1993**, *32*, 1111–1121.
[30] The energies of the charge-separated state were calculated by simply adding the reduction and oxidation potentials. It is safe to assume that the Coulombic terms in the present donor–acceptor systems are negligible, especially in solvents with moderate or high polarity, because of the relatively large edge-to-edge distances.
[31] D. Gust, T. A. Moore, A. L. Moore, *Res. Chem. Intermed.* **1997**, *23*, 621–651.
[32] a) H. Imahori, D. M. Guldi, K. Tamaki, Y. Yoshida, C. Luo, Y. Sakata, S. Fukuzumi, *J. Am. Chem. Soc.* **2001**, *123*, 6617–6628; b) D. M. Guldi, H. Imahori, K. Tamaki, Y. Kashiwagi, H. Yamada, Y. Sakata, S. Fukuzumi, *J. Phys. Chem. A* **2004**, *108*, 541–548.
[33] a) H. Imahori, K. Tamaki, Y. Araki, T. Hasobe, O. Ito, A. Shimomura, S. Kundu, T. Okada, Y. Sakata, S. Fukuzumi, *J. Phys. Chem. A* **2002**, *106*, 2803–2814; b) H. Imahori, K. Tamaki, Y. Araki, Y. Sekiguchi, O. Ito, Y. Sakata, S. Fukuzumi, *J. Am. Chem. Soc.* **2002**, *124*, 5165–5174.
[34] The temperature dependence prevents assignments regarding a superexchange or electron hopping mechanism. Considering the similar energetics we must also assume for **13b** an interplay between both mechanisms, but with a smaller activation barrier.
[35] F. D'Souza, G. R. Deviprasad, M. E. Zandler, M. E. El-Khouly, M. Fujitsuka, O. Ito, *J. Phys. Chem. A* **2003**, *107*, 4801–4807.
[36] These are even larger than those calculated for the dihedral angle between the two phenyl rings located at the two ends of the oligomer (28° for **13a** and 34° for **13b**).
[37] a) A. Osuka, K. Maruyama, N. Mataga, T. Asahi, I. Yamazaki, N. Tamai, *J. Am. Chem. Soc.* **1990**, *112*, 4958–4959; b) A. Helms, D. Heiler, G. McLendon, *J. Am. Chem. Soc.* **1992**, *114*, 6227–6238; c) F. Barigelletti, L. Flamigni, M. Guardigli, A. Juris, M. Beley, S. Chodorowski-Kimmens, J.-P. Collins, J.-P. Sauvage, *Inorg. Chem.* **1996**, *35*, 136–142; d) B. Schlicke, P. Belser, L. De Cola, E. Sabbioni, V. Balzani, *J. Am. Chem. Soc.* **1999**, *121*, 4207–4214; Polyenes: e) A. C. Benniston, V. Goulle, A. Harriman, J.-M. Lehn, B. Marczince, *J. Phys. Chem.* **1994**, *98*, 7798–7804; f) S. B. Sachs, S. P. Dudek, R. P. Hsung, L. R. Sita, J. F. Smalley, M. D. Newton, S. W. Feldberg, C. E. D. Chidsey, *J. Am. Chem. Soc.* **1997**, *119*, 10563–10564; Polyynes: g) A. Oskua, A. Tanabe, S. Kawabata, I. Yamazaki, Y. Nishimura, *J. Org. Chem.* **1995**, *60*, 7177–7185; h) V. Grosshenny, A. Harriman, R. Ziessel, *Angew. Chem.* **1995**, *107*, 1211–1213; *Angew. Chem. Int. Ed. Engl.* **1995**, *34*, 1100–1102; i) V. Grosshenny, A. Harriman, R. Ziessel, *Angew. Chem.* **1995**, *107*, 2921–2924; *Angew. Chem. Int. Ed. Engl.* **1995**, *34*, 2705–2708.
[38] C. M. Deber, P. D. Adawadkar, *Biopolymers* **1979**, *18*, 2375.

Received: June 15, 2004
Revised: October 27, 2004
Published online: January 5, 2005